

Revista Brasileira de Recursos Hídricos Brazilian Journal of Water Resources

Versão On-line ISSN 2318-0331 RBRH, Porto Alegre, v. 29, e37, 2024 Scientific/Technical Article

https://doi.org/10.1590/2318-0331.292420240042

Multi-model ensemble for long-term statistical trend analysis of observed gridded precipitation and temperature data in the São Francisco River Basin, Brazil

Conjunto de modelos para análise estatística de tendências de longo prazo de dados de precipitação e temperatura observados em grade na Bacia do Rio São Francisco, Brasil

Gabriel Vasco¹* , Rodrigo de Queiroga Miranda² , Jussara Freire de Souza Viana³ , Danielle Bressiani⁴ , Eduardo Mario Mendiondo⁵ , Richarde Marques da Silva⁶ , Josiclêda Domiciano Galvíncio³ , Samara Fernanda da Silva⁷ & Suzana Maria Gico Lima Montenegro³

¹Universidade Federal Rural de Pernambuco, Recife, PE, Brasil
 ²University of Guelph, Guelph, Ontario, Canada
 ³Universidade Federal de Pernambuco, Recife, PE, Brasil
 ⁴Universidade Federal de Pelotas, Pelotas, Brasil
 ⁵Universidade de São Paulo, São Carlos, SP, Brasil
 ⁶Universidade Federal da Paraíba, João Pessoa, PB, Brasil
 ⁷Universidade Federal do Oeste da Bahia, Barreiras, BA, Brasil

E-mails: gvasco23@gmail.com (GV), rodrigo.qmiranda@gmail.com (RQM), jussarafsouza@yahoo.com.br (JFSV), daniebressiani@gmail.com (DB), e.mario.mendiondo@gmail.com (EMM), richarde.marques@gmail.com (RMS), josicleda@gmail.com (JDG), samara.nanda@gmail.com (SFS), suzanam.ufpe@gmail.com (SMGLM)

Received: May 11, 2024 - Revised: August 05, 2024 - Accepted: August 19, 2024

ABSTRACT

For effective management practices and decision-making, the uncertainties associated with regional climate models (RCMs) and their scenarios need to be assessed in the context of climate change. This study analyzes long-term trends in precipitation and temperature data sets (maximum and minimum values) from the NASA, Earth Exchange Global Daily Downscaled Prediction (NEX-GDDP), under the São Francisco River Basin Representative Concentration Path (RCP) 4.5 and 8.5, using the REA (Reliable Ensemble Average) method. In each grid, the built multi-model was bias-corrected using the CMhyd software for annual, dry, wet, and preseason periods - for historical (1961-2005) and future (2006-2100) periods. The multi-model and four different methods, namely: The Mann-Kendall, Mann-Kendall pre-brightening test, bias-corrected pre-brightening, and Spearman correlation, were used to detect trends in precipitation, and minimum and maximum temperature. In the analysis of precipitation and temperature metrics, the results for the NRMSD showed that, in general, the CSIRO model presented more satisfactory results in all physiographic regions. Person's correlation coefficient showed a better adjustment of precipitation for the MIROC5, EC.EARTH and NORESMI1 models, in areas of sub-medium and upper São Francisco. For the minimum temperature, the CSIRO and NORESMI1 models showed the best fit, in general. At maximum temperature, the EC.EARTH and CSIRO models showed more satisfactory results. With regard to trend analysis, the results indicated an increasing trend in mean annual temperature and precipitation across the basin. When analyzed by subregion, the results show an increasing trend in monthly average minimum and maximum temperatures in the middle and lower SFRB, while average monthly rainfall increases during the rainy season and preseason in Upper São Francisco. The results of this research can be used by government entities, such as Civil Defense, to subsidize decision-making that requires actions/measures to relocate people/ communities to less risky locations to minimize risk or vulnerability situations for the population living nearby to the river.

Keywords: Brazil; Bias correction; Climate uncertainties; Nonparametric trend; Projections.

RESUMO

Para práticas de gestão e tomada de decisões eficazes, as incertezas associadas aos modelos climáticos regionais (MCR) e aos seus cenários precisam ser avaliadas no contexto das alterações climáticas. Este estudo analisa tendências de longo prazo em conjuntos de dados de precipitação e temperatura (valores máximos e mínimos) oriundos da NASA, da Earth Exchange Global Daily Downscaled



Prediction (NEX-GDDP), por meio do Caminho de Concentração Representativa (RCP 4.5 e 8.5), na Bacia do Rio São Francisco utilizando o método REA (Reliable Ensemble Average). Em cada grade, o multimodelo construído foi corrigido para períodos anuais, secos, chuvosos e pré-estação - para períodos históricos (1961-2005) e futuros (2006-2100), usando o software CMhyd. Para detectar tendências de precipitação e temperatura mínima e máxima na bacia, foram utilizados quatro diferentes métodos juntamente com o conjunto de dados que originou o multimodelo. Os quatro métodos utilizados foram: Mann-Kendall, teste de pré-clareamento de Mann-Kendall, pré-clareamento com correção de viés e correlação de Spearman. Na análise das métricas de precipitação e temperatura, os resultados do NRMSD mostraram que, de forma geral, o modelo CSIRO apresentou resultados mais satisfatórios em todas as regiões fisiográficas. O coeficiente de correlação de Person mostrou melhor ajuste da precipitação para os modelos MIROC5, EC.EARTH e NORESMI1, nas áreas do submédio e alto São Francisco. Para a temperatura mínima, os modelos CSIRO e NORESMI1 apresentaram o melhor ajuste, em geral. Na temperatura máxima, os modelos EC.EARTH e CSIRO apresentaram resultados mais satisfatórios. No que diz respeito à análise de tendência, os resultados indicaram uma tendência crescente na temperatura média anual e na precipitação em toda a bacia. Quando analisados por sub-região, os resultados mostram uma tendência crescente nas temperaturas médias mínimas e máximas mensais no médio e baixo SFRB, enquanto a precipitação média mensal aumenta durante a estação chuvosa e pré-estação no Alto São Francisco. Os resultados desta pesquisa poderão ser utilizados por entidades governamentais, como a Defesa Civil, para subsidiar tomadas de decisões que exijam ações/medidas de realocação de pessoas/comunidades para locais de menor risco para minimizar situações de risco ou vulnerabilidade para a população que vive nas proximidades do rio.

Palavras-chave: Brasil; Correção de viés; Incertezas climáticas; Tendência não-paramétrica; Projeções.

INTRODUCTION

The occurrence of climate change, which can change both the frequency and intensity of climate events, has exposed a wide range of impacts on food production, water supply, and the environment, and are one of the major challenges for environmental and water resource management in the 21st-century (Gebrechorkos et al., 2019; Liu et al., 2017).

Recent climate change has altered precipitation variability – spatial and temporal distribution, annual and seasonal patterns, and increased temperature (in the order of 1.1 °C and 6.4 °C throughout the 2st-century) in different parts of the world, which have received much attention by researchers and water and environmental policymakers (Banerjee et al., 2020; Panda & Sahu, 2019).

More severe extreme events will occur due to more severe climate change, causing significant consequences. In the São Francisco River Basin, heat waves last several days to weeks with temperatures often exceeding 35 °C and growing in frequency. Intense precipitation events, producing over 50 mm of rain per hour, are increasingly common, leading to flooding. Prolonged droughts can last for months to years, with significant water shortages and reduced river flows becoming more frequent and severe due to climate change.

Therefore, given the water scarcity, the prediction of climatic extremes is essential to analyze the impacts of climate change on the environment and in the numerous agricultural irrigation projects (Assis et al., 2015).

The analysis of hydrometeorological time series trends gained importance in recent years, due to the impacts that are becoming very evident in the environment, in the hydrological cycle on a global, regional, and local scale, and in the social and economic well-being (Kotir, 2011; Mallakpour et al., 2022; Nascimento do Vasco et al., 2019). In addition, these analyses are relevant to assessing climate-induced changes and planning viable adaptation strategies related to these changes.

Precipitation and temperature are two of the most important variables in the field of climate sciences and hydrology often used to trace the extent and magnitude of climate changes and variability, as these physical parameters determine the environmental condition of the particular region that affects agricultural productivity for food provision (Carvalho et al., 2020).

The spatial and temporal variability of precipitation and temperature is notorious in several studies already pulsing around the world, studying patterns of trends concerning climate change, based on the observed data available for longer periods (Buri et al., 2022; Hundecha & Bárdossy, 2005; Isotta et al., 2019; Kanda et al., 2020; Li et al., 2022; Mallakpour et al., 2022).

Recent research indicates that the São Francisco River basin has experienced a notable increase in temperature extremes, with more frequent and intense heatwaves observed over recent decades (Marengo, 2014). Concurrently, changes in precipitation patterns have led to more pronounced extremes, including increased frequency of heavy rainfall events and prolonged dry spells. For instance, analyses have shown that intense rainfall events are becoming more common, contributing to higher variability in water availability and impacting river flow dynamics. These observed trends underscore the importance of incorporating current climate extremes into future projections, as they offer valuable insights into how ongoing climatic shifts may influence hydroelectric power generation and water resource management in the basin.

In Brazil, scientific efforts to understand hydrometeorological aspects of the SFRB have been carried out, given its relevance to the Brazilian semiarid (Bezerra et al., 2019; Montenegro & Ragab, 2012; Ribeiro Neto et al., 2016), as there are still few detailed studies on the patterns of the long-term trend for precipitation and temperature (minimum and maximum) in the São Francisco River basin, which has suffered from systematic drought problems in recent years, leading to serious threats to water and environmental security (Assis et al., 2015; Bezerra et al., 2019; Fonseca et al., 2019; Silveira et al., 2016; Souto et al., 2019; Teixeira et al., 2021).

In this context, the SFRB is being considered as one of the areas of study for the development of an integrated water resource management model in climate change scenarios, as part of the ongoing BRICS-STI multilateral project. Therefore, given the importance of redefining water resource management policies and making the system more resilient to the challenges of climate change, the main objective of this study is to analyze the seasonality, variability, and long-term trend of precipitation and temperature data available in the SFRB, using four different trending methods.

MATERIALS AND METHODS

Study area

The present study was carried out in the São Francisco River basin, located entirely in Brazil, covering an area of 636.920 km² (7.5% of the Brazilian national territory). It drains areas of seven federative units, with an extension of approximately 2.700 km, discharging 94 000 000 m³ annually. The basin shows fragments of different biomes, Atlantic forest, Caatinga, coastal, and Cerrado that cover practically half of the basin area, in addition to the predominance of soils with an aptitude for irrigated agriculture.

The average annual evapotranspiration is 896 mm, presenting high values between 1400 and 840 mm, due to the high temperatures (22-32 °C), the intertropical geographical location and the reduced cloudiness, high incidence of solar radiation, and the relatively high annual evaporation rates of around 2300 to 3000 mm. The area has an irregular distribution of rainfall throughout the year, from November to January, the wettest quarter, contributing 55 to 60% of annual rainfall, while the driest quarter is from June (Marques et al., 2019).

The basin is an area of strategic economic and development importance, with socioeconomic disparities between the sub-basins, with emphasis on predominantly urban uses and occupations in the highest part, and agricultural and mining activity spread throughout the basin, in addition to a robust industrial park, covering the metallurgical, textile, food, and chemical companies areas (Bezerra et al., 2019). In addition, the Lower Middle San Francisco is vulnerable to the occurrence of severe droughts, usually associated with strong El Niño, besides being challenged by water conflicts for multiple uses (Bezerra et al., 2019; Lucas et al., 2021). The study area encompasses a significant hydrographic basin known for its critical hydroelectric plants, notably Sobradinho and Xingó. These plants play a crucial role in the region's energy production and water management. Sobradinho Dam, located on the São Francisco River, creates one of the largest reservoirs in Brazil and is vital for regulating water flow and generating electricity. Xingó Dam, situated downstream, is also a key facility, contributing to energy production and flood control. Together, these hydroelectric plants are central to the basin's infrastructure, influencing local ecosystems, water availability, and regional development (Figure 1).

Data description

A 44-year dataset (1961-2005) was obtained through two databases, (i) daily rainfall data (mm) through the APAC website (Pernambuco State Agency for Water and Climate; Agência Pernambucana de Águas e Clima, 2024), and ANA (National

Water and Basic Sanitation Agency; Agência Nacional de Águas e Saneamento Básico, 2024); (ii) complete meteorological data such as precipitation (mm), solar radiation (MJ/m²), relative humidity or dew point temperature (%), average air temperature, maximum and minimum air temperatures (°C), and wind speed (m/s) through the INMET (National Institute of Meteorology) database (Instituto Nacional de Meteorologia, 2024).

For the preparation of grid data, daily rainfall records of rainfall stations in Brazil and APAC stations (for the State of Pernambuco) were used. The grid data set was developed after the quality control of the rainfall stations, performed as follows: (i) replace all missing values (currently coded as -99.9) into an internal format that the software recognizes (i.e., NA, not available) and (ii) replace all unreasonable values into NA.

"Further, a 149-year historical climate dataset was used on a $0.25^{\circ} \times 0.25^{\circ}$ grid for precipitation and a $1^{\circ} \times 1^{\circ}$ grid for temperature. This data was shared by the Indian team as part of the BRICS multilateral research project".

The multi-model ensemble approach

Multi-model ensembles (MMEs) are widely employed in short-range climate forecasting to reduce uncertainties inherent in GEOS-5 Atmosphere-Ocean General Circulation Model (AOGCM) simulations and projections (Ahmed et al., 2020). These uncertainties stem from factors such as: measurement errors, stochastic variability, and systematic biases across multiple climate models (Clark et al., 2016). To address these uncertainties, various Regional Climate Models (RCMs) and emission scenarios are integrated and termed as Multi-Model Ensemble (MME). For this, it was used the Reliability Ensemble Averaging (REA) methodology, which measures multimodel uncertainty in the form of performance to then increase confidence when projecting climate data into the future.

Aiming to identify the optimum number of AOGCMs required for an MME from a pool of AOGCMs ranked based on their performance in simulating past observed climates, this work was used a total of nine driving CMIP5 AOGCMs (CAnESM2, CM5A-MR, CSIRO, EC-EARTH, GFDL-ESM2M, HadGEM2-ES, MIROC5, NORESM1, and SHMI-ESM), and two emission scenarios (RCP 4.5 and RCP 8.5) (Thomson et al., 2011; Schwalm et al., 2020), to represent the present-day climate factually and obtain comparing GCM simulations with observed climate by considering performance measures.

The process of integrating an ensemble of models was done by taking a simple arithmetical average or by following a weighting procedure developed on the performance indicators of the RCMs simulating historic climate data, and BIAS Correction.

1. Performance indicators

To evaluate RCMs' ability to match the actual climate, the performance indicators used in this work were Normalized Root Mean Square Deviation (NRMSD) and Pearson Correlation Coefficient (CC), whose mathematical equations for each indicator as well as their ideal values are summarized in Table 1. For the calculation of performance indices, average monthly precipitation, and temperature data sets of observed (IMD) and simulated (RCM) values are used

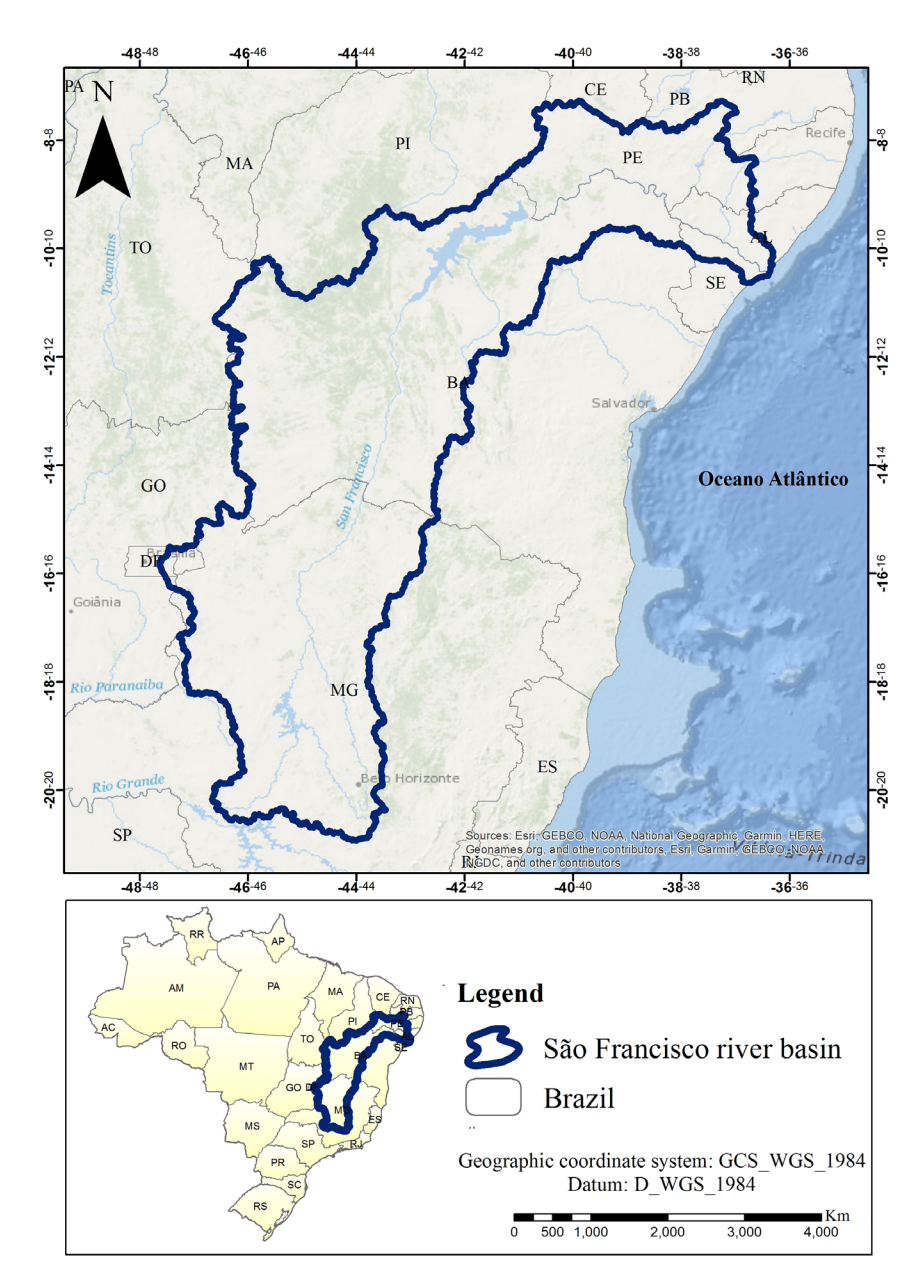


Figure 1. Geographic location map of the São Francisco River basin, Brazil.

Table 1. The mathematical equations and ideal values of performance metrics.

S. No.	Performance Metric	Equation	Ideal Value
1	Normalized Root Mean Square Deviation (NRMSD)	$\frac{\sqrt{\frac{1}{T}}\sum_{i=1}^{T}(X_i - Y_i)^2}{\bar{X}}$	0
2	Pearson Correlation Coefficient (CC)	$\frac{\sqrt{\frac{1}{T}} \sum_{i=1}^{T} (z_i - \overline{z}) (y_i - \overline{y})}{(T - 1)\sigma_{obs}{}^{\sigma} sim}$	1

for the period 1961-2005. The observed and simulated values of the respective datasets are x_i and y_i . The mean of observed and simulated values is denoted by x-and y-. The number of datasets is

denoted by T. The standard deviations of observed and simulated values are denoted by σ_{obs} and σ_{sim} , respectively.

2. Normalization Technique

Table 2. Methodology of entropy technique.

Step	Description	Mathematical expression
1	Normalize the payoff matrix if required	k_{aj}
2	Entropy for each indicator	$En_j = -\frac{1}{ln(T)} \sum_{a=1}^{T} k_{aj} ln(k_{aj})$, for $j = 1,, Ja$ is index for GCMs; $(j=1,2,,j)$ where J is number of indicators; T represents total number of GCMs.
3	Degree of diversification	$Dd_{j} = 1 - En_{j}$
4	Normalize the weight of indicators	$r_{j} = \frac{Dd_{j}}{\sum_{j=1}^{j} Dd_{j}}$

The mathematical representation for normalization is shown in Equation 3 (Patakamuri et al., 2020), which helps the conversion of different proportionate indicators into the same space.

$$k_{aj} = \frac{K_j(a)}{\sum_{a=1}^{N} k_j(a)} \tag{1}$$

where $k_j(a)$ is the value of indicator j for RCM a; N represents the total number of RCMs.

3. Entropy technique

The mathematical representation of the entropy technique is shown in Table 2.

4. Methodology of weighted average technique

In this step normalize the payoff matrix if required, where the utility of RCM (V_a) is calculated by Equation 4.

$$V_a = \left[\sum_{j=1}^j r_j k_j \right] \tag{4}$$

here, k_j represents the value of indicator j for RCM, and r_j denotes the weight assigned to indicator j. A higher V_a indicates a suitable RCM.

For each RCM, the strengths, weaknesses, and net strengths were calculated based on individual ranking techniques and were integrated to form a single ranking pattern based on an individual ranking analysis (Morais & Almeida, 2012). Weights were assigned to all RCMs using a weighted average method considering the net strengths. All nine ranked RCMs for the precipitation and temperature datasets at each grid point were ensembled by assigning weights to reduce uncertainty.

Non-parametric trend tests

Detection of pattern changes and the existence of trends in hydrometeorological phenomena have been extensively investigated in the study of hydrology, climatology, and meteorology, with particular emphasis on non-parametric tests, notably the classic Mann-Kendall (MK) test and Sen's slope estimator (Achite et al., 2021; Hussain et al., 2022; Sarioz et al., 2024). These authors, along with Achite et al. (2023) and Ahmed et al. (2022) address

the limitations of the MK method, especially regarding the serial independence of the time series and present more innovative methods. Among these methods, the following were described: Innovative Trend Analysis (ITA), Innovative Polygon Trend Analysis (IPTA), and Innovative Triangular Trend Analysis (ITTA). In the present work, the usual tests were chosen, as they were agreed upon within the scope of the multilateral project. According to the findings of Sarioz et al. (2024), the more innovative methods demonstrate greater sensitivity in detecting trends compared to the classic Mann-Kendall and Spearman Rho methods.

Thus, the Mann-Kendall Test (MK), Spearman's correlation (Spearman), Pre-Whitening Mann-Kendall Test (PWMK), and Bias-Corrected Pre-Whitening Test (BCPW) were adopted in the present study. In our analysis, we employed the Mann-Kendall test to evaluate the presence of trends in the data. To determine whether the observed trends were statistically significant, we set the significance level (a) at 0.05. This threshold indicates that we accept a 5% chance of incorrectly rejecting the null hypothesis (which posits that there is no trend) when it is actually true. By using this level of significance, we aimed to balance the risk of Type I and Type II errors in our trend analysis. More details on the methodologies employed can be found in Buri et al., (2022). These tests are widely used to detect trends in non-normally distributed environmental and hydrometeorological data (van Giersbergen, 2005; Santos et al., 2020; Patakamuri et al., 2020; Wang et al., 2020). The determination of the values for the adopted tests was conducted using R software (modifiedmk package; R Core Team, 2024).

Future climate change scenarios

To project the possible future impacts on hydrological processes due to climate change in the São Francisco River basin, simulated climate data of NASA Earth Exchange Global Daily Downscaled Projections (NEX-GDDP), under two Representative Concentrative Pathways (RCP)¹: RCP 4.5 and RCP 8.5. This data was made available by the Indian team, as part of the ongoing multilateral BRICS research project, titled "Integrated Water Management Model for Brazil, India, and South Africa under climate change scenarios".

 $^{^{1} \}mbox{These RCPs}$ are based on assumed natural and anthropogenic radiative forcing through the end of the 21^{st} -century.

Statistical bias correction method

In this work, the Linear Scaling (LS) method was applied to bias-correct downscaled precipitation and temperature data of an ensemble model from nine climate models. This technique was chosen after a literature review (Teutschbein & Seibert, 2012), which evaluated five bias correction methods for precipitation and four bias correction techniques for temperature, and according to other studies (Andrade et al., 2021), linear scaling is suitable both for precipitation and temperature.

The trendline correction procedures are used to minimize the discrepancy between observed and simulated climatic variables in a daily time step so that the hydrological simulations conducted by corrected simulated climatic data correspond to the simulations using observed climatic data reasonably well (Rathjens et al., 2016). To this end, the *Climate Model Data for Hydrologic Modeling* (CMhyd) (Rathjens et al., 2016), can be applied to extract and correct (correct) data obtained from global and regional climate models with the observed data, given the difficulty in using simulated climatic data as direct input data for hydrological models.

For bias removal for the projected climatic data, the CMhyd model needs observed data, historical data, and Climate Change Projections for South America, adopting the *Linear Scaling (LS)* technique, which uses monthly correction values established in the differences between observed and historical simulated data (Andrade et al., 2021; Teutschbein & Seibert, 2012, 2013), according to below-given Equations 5 to 8.

$$P^{*}_{contr}(d) = P_{contr}(d) \cdot \left[\frac{i_{m}(P_{obs}(d))}{i_{m}(P_{contr}(d))} \right]$$
 (5)

$$P_{scen}^{*}(d) = P_{scen}(d) \cdot \left[\frac{i_{m}(P_{obs}(d))}{i_{m}(P_{contr}(d))} \right]$$
(6)

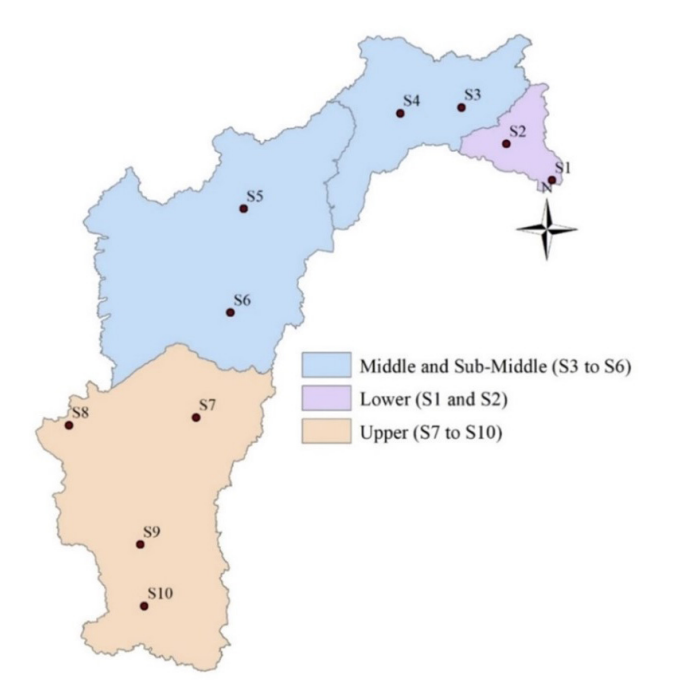


Figure 2. Spatial distribution of selected stations along the São Francisco River basin.

$$T_{contr}^{*}(d) = T_{contr}(d) + \mu_{m}(T_{obs}(d)) - \mu_{m}(T_{contr}(d))$$
 (7)

$$T_{\text{scen}}(d) = T_{\text{scen}}(d) + \mu_{\text{m}}(T_{\text{obs}}(d)) - \mu_{\text{m}}(T_{\text{contr}}(d))$$
(8)

where: P(d) and T(d) are daily precipitation and temperatures, respectively; µm is the monthly mean value of the variable m; and "contr", "scen" and "obs", refer to the control (baseline period), scenarios and observed data, respectively.

In the LS approach, bias-corrected simulation data should agree, in their monthly average values, with the observed data and a factor based on the ratio of long-term monthly average observed and control run data is used for adjustment of precipitation and temperature variable, being expected that these factors will continue unvaried under future conditions of the study area basin.

The observed precipitation and temperature data comprised ten representative stations (Figure 2), distributed throughout the SFRB, both chosen based on the Principal Component Analysis (PCA) (Edwards & Cavalli Sforza, 1965).

This PCA approach is determined as a linear combination of the original variables, to help reduce the dimensionality of the data set and determine the variables that better explain the variability of the data with a lesser number of variables. The simulated historical data corresponding to the same period came from the historical series of the ensemble climate data.

Bilinear interpolation and IDW

To bring the same resolution for both precipitation and temperature datasets, a bilinear-interpolation technique was applied. For generating spatial plots, inverse distance weighting (IDW) geostatistical interpolation explicitly technique (Bartier & Keller, 1996), which assumes that things that are close to one another are more alike than those that are farther apart, was used by considering the Z-value of respective trend tests.

To predict a value for any unmeasured location, IDW uses the measured values surrounding the prediction location. The measured values closest to the prediction location have more influence on the predicted value than those farther away (Biswas et al., 2020). The IDW technique assumes that each measured point has a local influence that diminishes with distance. It gives greater weights to points closest to the prediction location, and the weights diminish as a function of distance, hence the name inverse distance weighted.

The annual analysis was carried out for the entire study area. However, given the great heterogeneous along the basin with four climatic types, trend analysis in the dry, rainy, and pre-season periods was performed, in a sub-region subdivided by Lower (S1 and 2), Middle and Sub-Middle (S2-S6), and Upper São Francisco (S7-S10), as shown in Table 3, and spatially scattered in Figure 2.

The methodology followed in this study, as shown in Figure 2, was demonstrated at a climate model grid point, and the same procedure was followed for the remaining grid points of the study area.

RESULTS

At each grid point, the net resistance of each RCM was evaluated using the Root Mean Square Deviation Normalized

Table 3. Sub-regions and stations for trend analysis in the dry, rainy, and pre-season periods.

Region (stations)	Season	Period	Chosen month
Lower (S1 and S2)	Dry	May – October	July
	Rainy	November – April	January
		Pre-season	October
Middle and Sub-Middle (S3-S6)	Dry	June – November	September
	Rainy	December – May	February
		Pre-season	November
Upper (S7-S10)	Dry	September – February	November
	Rainy	March-August	May
		Pre-season	February

Source: Adapted from Galvíncio (2000) and Siqueira et al. (2022).

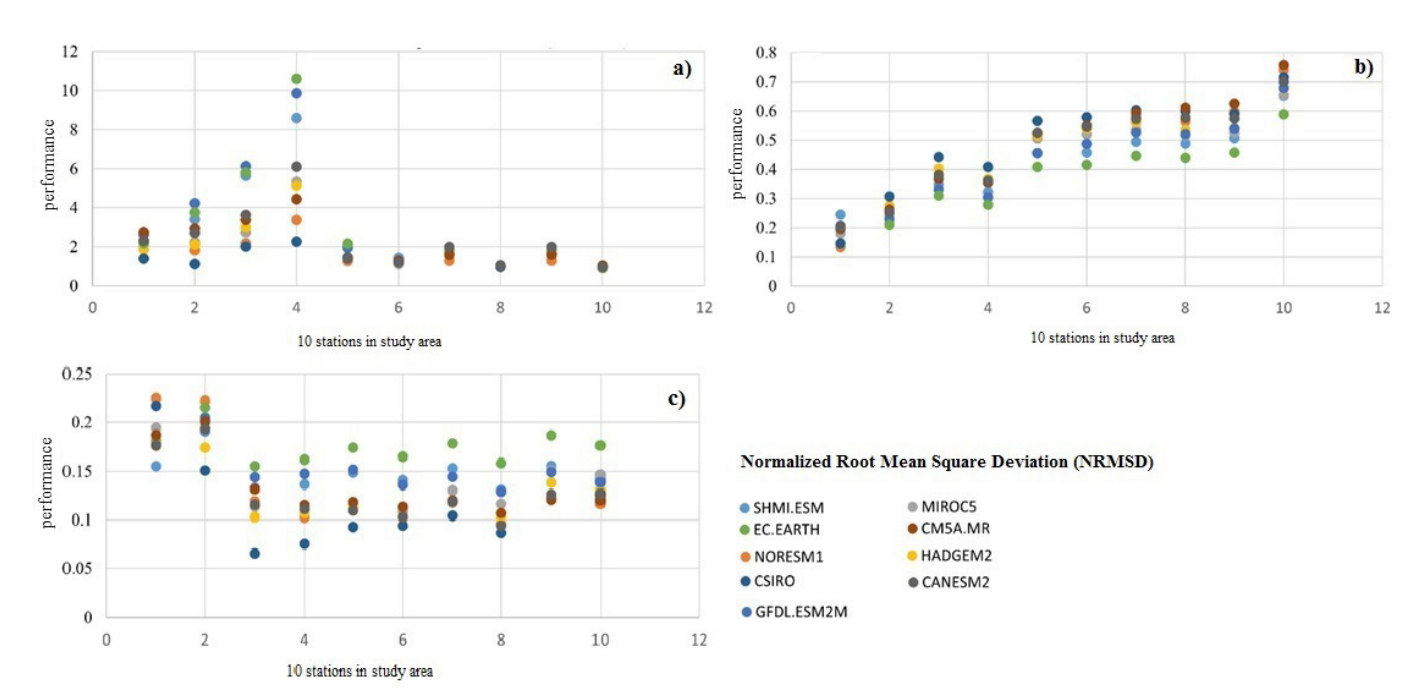


Figure 3. Performance analysis of NRMSD metric of precipitation (a), and minimum (b) and maximum temperature (c) for 9 RCMs in 10 points.

Mean Square Deviation (NRMSD) and Pearson Correlation Coefficient (CC) performance indicator, suitable for comparing data sets or models with different scales. In this case, precipitation and temperature data were used, as shown in Figure 3 and 4. These weighting schemes were applied to find the best historical fit of three climate variables (precipitation and minimum and maximum temperature). Regarding the NRMSD metric relating to precipitation, a greater range of variation in model results is observed in the physiographic regions of the lower and, especially, the middle São Francisco, with better results coming from the CSIRO model in all physiographic regions (Figure 3). In general, all models presented excellent results in relation to this index, both for minimum and maximum temperatures, with values below 0.8 and 0.25, respectively.

In Figure 4a it is possible to observe that there is a better fit of the MIROC5, EC.EARTH and NORESMI1 models, with values above 0.6, in stations that are located in the sub-medium and upper São Francisco. In other stations, the models presented an adjustment below 0.5. As for temperatures (Figure 4b-c), a

greater variation can be seen in the adjustment of the data to the minimum, where the models present different behaviors in all the stations analyzed. However, it is possible to observe that CSIRO and NORESMI1 showed a higher correlation in most stations, in the low, medium and sub-medium areas, with a variation above 0.6. The correlation in maximum temperature (Figure 4c) indicated a good fit of the data for all climate models analyzed at stations located in the lower and middle São Francisco, with values above 0.58. In other stations (sub-medium and high), the adjustment for all climate models was below 0.6. For maximum temperature, the EC.EARTH and CSIRO climate models, in general, presented better results.

Figure 5 represents the model weights (Va) for precipitation, minimum and maximum temperature based on their individual performance to create the multi-model, from of the nine climate models analyzed for the ten points arranged over the basin (Figure 2). Each point on the graph represents the nine climate models and the weights of each of them. The y-axis represents the weight of each model in creating the multi-model, and the

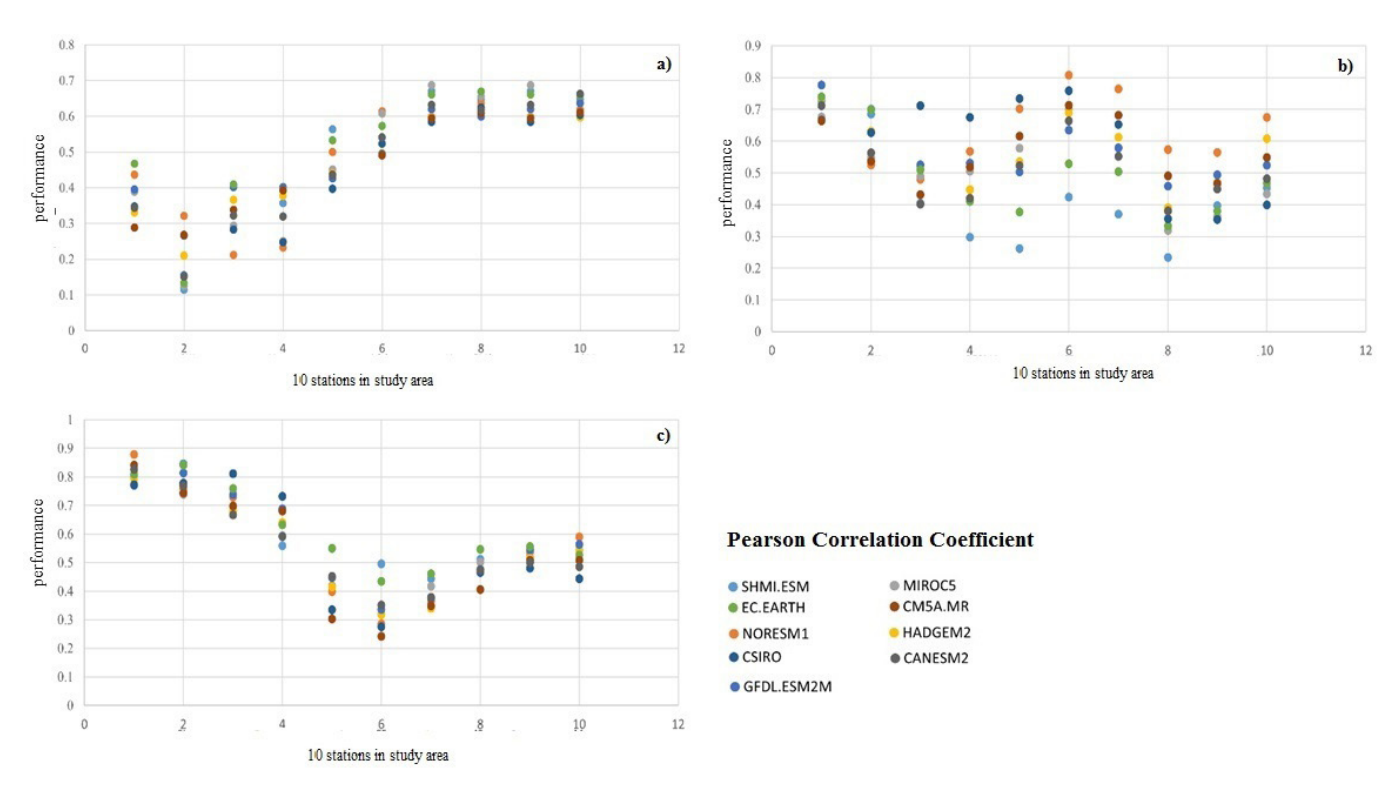


Figure 4. Performance analysis of Pearson Correlation Coefficient (CC) metric of precipitation (a), minimum (b) and maximum temperature (c) for 9 RCMs in 10 points.

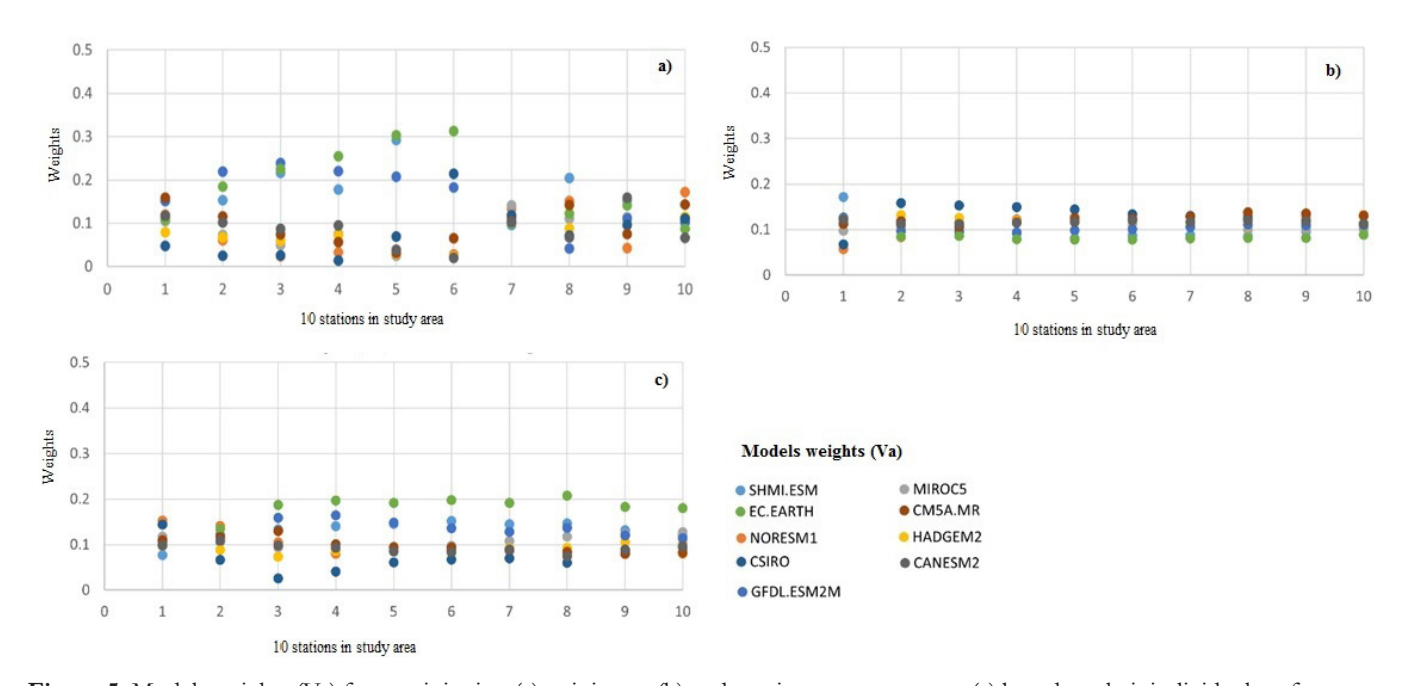


Figure 5. Models weights (Va) for precipitation (a), minimum (b) and maximum temperature (c) based on their individual performance to create the multi-model.

x-axis is each of the selected points placed on the basin (Figure 2). The results show that the EC.EARTH model had a greater weight for precipitation (Figure 5a-c) and maximum temperature, differing from the minimum temperature (Figure 5b), where in general, the CSIRO and CM5A.MR presented greater weight for creating the multi-model.

Annual precipitation trend analysis

Table 4 shows the annual variation in average precipitation for different periods in two climate scenarios (RCP4.5 and RCP8.5), in the analyzed sub-regions of the São Francisco basin (Figure 2). According to the results obtained, for the RCP 4.5 scenario there

Table 4	Variation of	annual average	precipitation	for different	periods und	ler the RO	P 4 5 and	RCP 8.5 scenarios.	
Table T.	vanauon or	aimuai avciago	DICCIDICATION	ioi unitetent	Denous une		T.J and	i ivoi olo sechanos.	

C : -	C4 - 4:	D	1961 - 2020	2021 - 2059	2060 - 2100	V1	V2	V3
Scenario	Station	Region	(T1) mm	(T2) mm	(T3) mm	(T2-T1) mm	(T3-T2) mm	(T3-T1) mm 153.59 112.02 132.60 144.19 88.39 170.34 55.35 144.06 97.88 -4.72 240.90
	S1	T.T.	3609.53	3770.70	3763.13	161.17	-7.57	153.59
	S2	Upper	1388.90	1475.72	1500.92	86.81	25.21	112.02
	S3		1071.25	1134.01	1203.85	62.76	69.84	132.60
	S4	MSM	1194.32	1267.09	1338.51	72.77	71.42	144.19
RCP 4.5	S5	MSM	983.62	1003.51	1072.00	19.89	68.50	88.39
KCP 4.5	S6		1034.00	1104.90	1204.34	70.90	99.44	170.34
	S7		728.87	748.31	784.22	19.45	35.91	55.35
	S8	Lower	1283.80	1368.45	1427.85	84.65	59.40	144.06
	S9		2041.58	2088.41	2139.46	46.83	51.06	97.88
	S10		813.25	794.30	808.53	-18.94	14.22	-4.72
	S1	11	3599.59	3791.37	3840.49	191.78	49.12	240.90
	S2	Upper	1389.79	1506.43	1596.01	116.64	89.58	206.22
	S3		1072.85	1193.43	1319.57	120.58	126.14	246.72
	S4	MCM	1189.64	1324.11	1461.23	134.47	137.12	271.59
DCD0 F	S5	MSM	986.07	1047.81	1124.21	61.74	76.41	138.14
RCP8.5	S6		1040.53	1158.44	1244.76	117.91	86.32	204.23
	S7		726.44	757.75	810.21	31.31	52.46	83.77
	S8	T owner	1286.62	1412.40	1560.88	125.78	148.48	274.26
	S9	Lower	2041.58	2088.41	2139.46	46.83	51.06	97.88
	S10		813.25	794.30	808.53	-18.94	14.22	-4.72

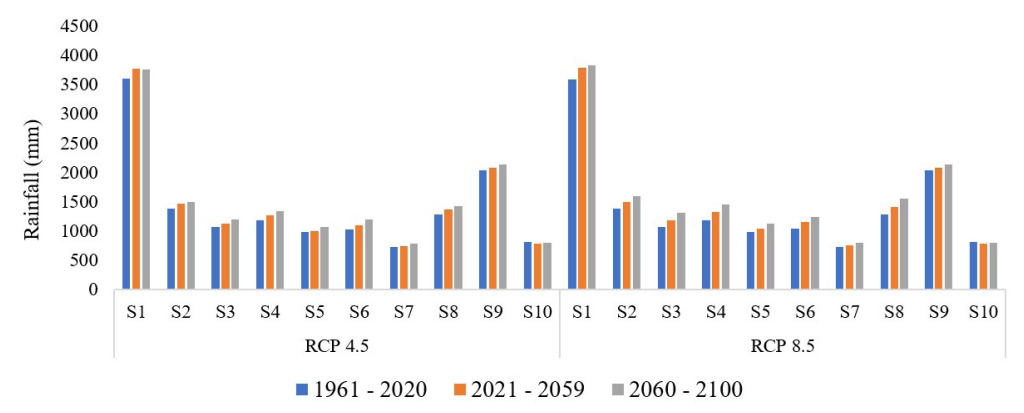


Figure 6. Mean annual precipitation (mm) for the entire São Francisco River basin.

will be a tendency for precipitation to increase in practically all stations in the basin analyzed, except for S1 and S10, which showed a slight tendency for rainfall to decrease in different periods. In the RCP 8.5 scenario, the same trend of increased rainfall remains, but with higher rates, with the exception of station S10 located in lower São Francisco, which also projects a slight decrease in rainfall in the location, maintaining the projection of scenario 4.5.

Figure 6 illustrates the annual average precipitation over the entire São Francisco River from the perspective of the two future scenarios analyzed (RCP 4.5 and 8.5) and the current period observed. Projections in both scenarios indicate an increase in precipitation throughout the basin, with regions with higher rainfall rates than others. Due to the action of different large, meso, and local scale meteorological systems (Oliveira et al., 2017), the rainfall regime in the basin presented high spatiotemporal variability (geographically and seasonally), indicating a well-defined annual cycle with wet and dry periods (Freitas et al., 2022). The SFRB will

certainly experience more rainfall and greater temperatures in the future for both emission scenarios, based on the results obtained in this study, which report a trend of increasing average annual precipitation in the two future periods under the RCP 4.5 and RCP 8.5 scenarios compared to the historical period (Figure 6). This increasing trend is influenced by tropical climatic phenomena and the El Niño phenomenon, which interferes in the rainy season between the years (Andreoli & Kayano, 2005; Ferreira et al., 2021).

This increasing trend of precipitation when evaluated through four (4) non-parametric trend tests adopted in this study (Figure 7), showed, as the Mann-Kendall Test (MK) (a) for example, an increasing trend in the Upper, Medium, and Sub-medium São Francisco. A high correlation was evidenced by the Spearman correlation test (b), even after eliminating possible adverse effects of autocorrelation in the MK test and Spearman's rho trend tests, through the Mann-Kendall Test of Pre-Whitened (PWMK) test (c).

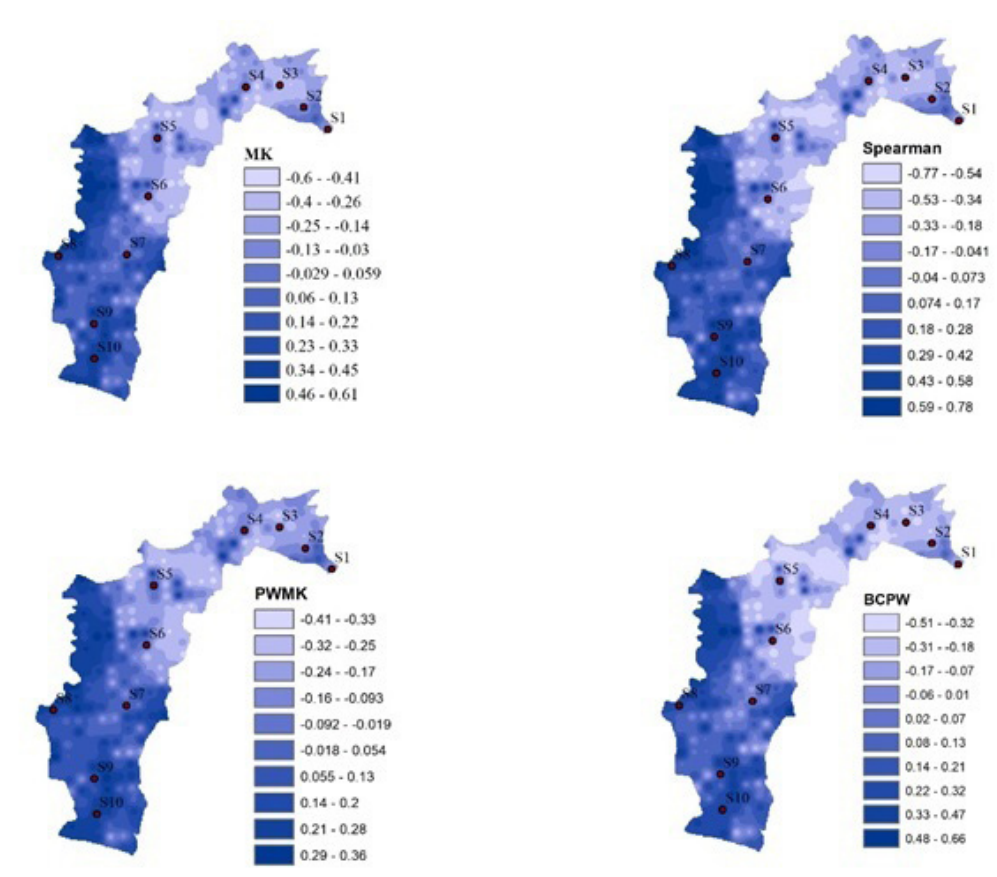


Figure 7. Spatial variation of Z-value and trend showing grid points in four trend tests –Mann-Kendall Test (MK) (a), Spearman correlation test (b), Pre-Whitened (PWMK) test (c) and Bias-Corrected Pre-Whitening Test (BCPW) (d)– of precipitation data annual period over the São Francisco River Basin.

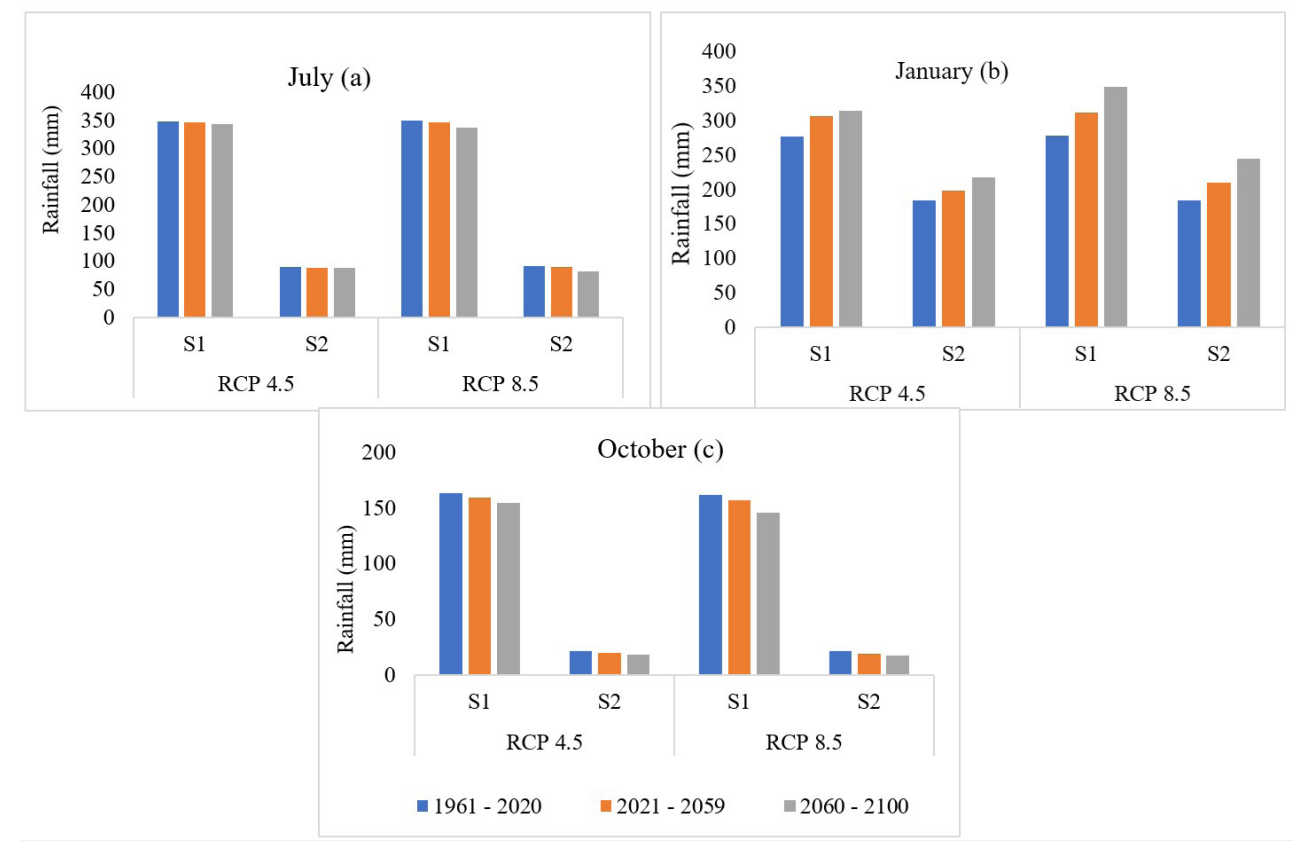


Figure 8. Station-wise means monthly precipitation (mm) in the dry (a), rainy (b), and pre-season (c) periods over Lower São Francisco.

Monthly precipitation trend analysis

Figures 8a-c shows the monthly average precipitation in the São Francisco basin by climatic periods, namely: dry (a), rainy (b) and pre-season (c), in the physiographic region of the lower São Francisco. In the lower São Francisco region, affected by easterly wave disturbances and sea and land breezes (Reboita et al., 2010), the lowest precipitation values were observed in the pre-season period, which jointly with the dry period, recorded lower precipitation values when compared to the observed period, differently from the rainy period, which observed an increase in means monthly precipitation for both RCPs.

Figures 9a-c shows the monthly average precipitation in the São Francisco basin by climatic periods, namely: dry (a), rainy (b) and pre-season (c), in the physiographic region of the Middle and Sub-Middle São Francisco. These results showed a decreasing trend in rainfall in the dry and pre-season periods, the precipitation values in two future periods will decrease if compared to those historically observed in both RCPs. Similar negative trend or decreasing trends in annual precipitation were detected by (Moncunill, 2006) while analyzing the two river basins in the Sertão region of the State of Pernambuco in the years between 1964-2004, and in the State of Ceará, using 23 rainfall stations between 1974 and 2003, respectively.

The greatest variations occurred in the rainy season, with emphasis on the predominance of positive anomalies were also

reported (Sales et al., 2015), in their study on precipitation and temperature projections for the Brazilian Northeast, considering the CMIP5 models and the RCP8.5 scenario. These results' alignment, also can be seen with the report of the Brazilian Panel on Climate Change (Brasil, 2013), stating that the Northeastern semiarid region of Brazil is likely to have its precipitation reduced by 20% in 2040, and highlighting that the more intense in the Northern part of the region, mainly located in the State of Pernambuco (Assis et al., 2022). Differently in the rainy period, observed precipitation values for future periods were high in both RCPs.

Based on the exposed above, it is noted that the reported reduction in rainfall in the Middle and Sub-Middle São Francisco regions corroborates with the past aforementioned studies, a persisting problem in the semiarid region of the Brazilian Northeast, which is currently facing its worst drought in decades (Assis et al., 2022).

In the Upstream São Francisco, in Minas Gerais State, where the weather systems are associated with the South Atlantic Convergence Zone (SAZC) and isolated convection (Siqueira et al., 2022), the precipitation monthly averages presented in Figure 10, showed lowest precipitation values for two future periods will be observed in the pre-season period, which also showed an increasing trend in the precipitation values in both future periods and RCPs. While for the dry and rainy periods, there will be decreasing trends, in two considered scenarios.

To face these upcoming water demand increases in the Upper and Middle (and water scarcity in the sub-Middle and Lower) due to

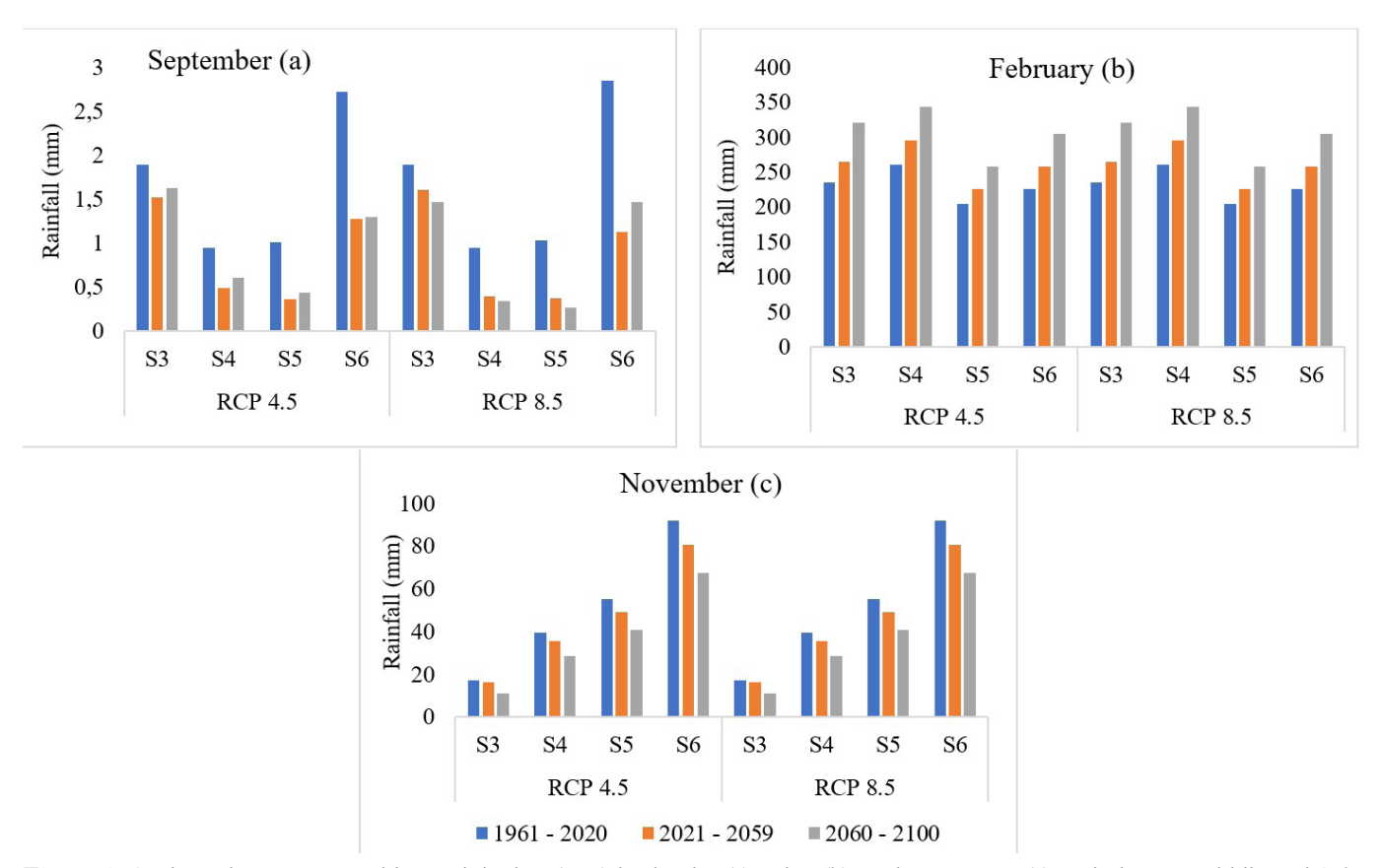


Figure 9. Station-wise mean monthly precipitation (mm) in the dry (a), rainy (b), and pre-season (c) periods over Middle and Sub-Middle São Francisco.

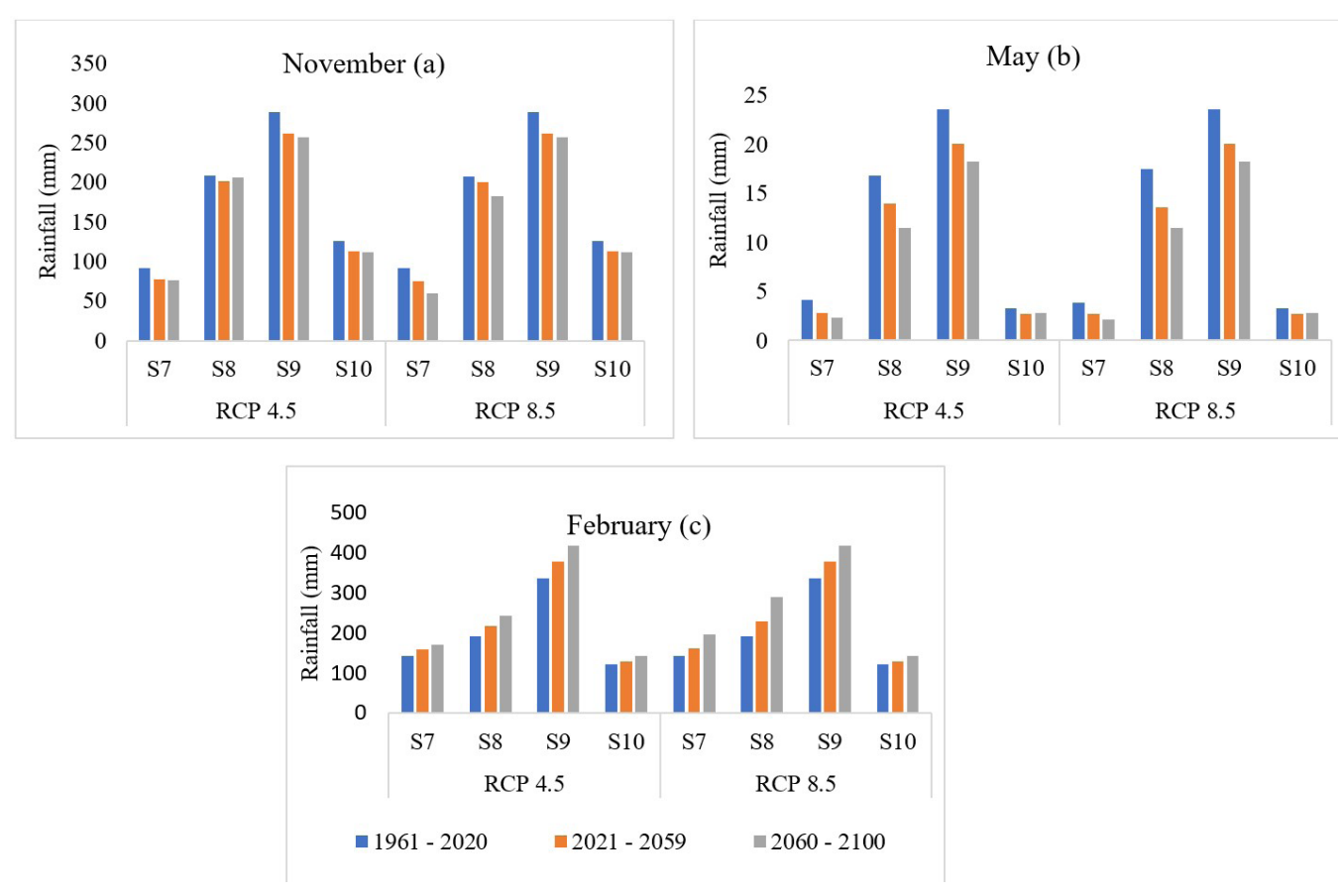


Figure 10. Station-wise mean monthly precipitation (mm) in the dry (a), rainy (b), and pre-season (c) periods over Upper São Francisco.

Table 5. Variation of annual average minimum temperature for different periods under the RCP 4.5 and RCP 8.5 scenarios.

C : -	Ctation.	Region	1961 - 2020	2021 - 2059	2060 - 2100	V 1	V2	V3
Scenario	Station		(T1) °C	(T2) °C	(T3) °C	(T2-T1) °C	(T3-T2) °C	(T3-T1) °C
	S1	T.T	21.74	22.97	23.53	1.23	0.57	1.79
	S2	Upper	22.24	23.59	24.29	1.34	0.70	2.05
	S3		21.36	22.62	23.29	1.26	0.66	1.93
	S4	мем	21.69	22.95	23.66	1.26	0.71	1.97
DCD 4 5	S5	MSM	20.04	21.31	22.05	1.27	0.74	2.01
RCP 4.5	S6		19.83	21.17	21.93	1.34	0.76	2.10
	S7		18.56	19.93	20.68	1.37	0.75	2.13
	S8	Lower	17.20	18.61	19.42	1.41	0.81	2.22
	S9		17.09	18.45	19.21	1.37	0.75	2.12
	S10		16.01	17.42	18.18	1.41	0.76	2.17
	S1	Upper	21.74	23.24	24.44	1.50	1.20	2.69
	S2		22.24	23.90	25.64	1.66	1.74	3.40
	S3		21.36	22.93	24.57	1.57	1.64	3.21
	S4	MSM	21.69	23.28	25.03	1.58	1.75	3.33
DCD 0.5	S5	MSM	20.05	21.65	23.52	1.60	1.87	3.47
RCP 8.5	S6		19.84	21.52	23.48	1.68	1.96	3.64
	S7		18.57	20.26	22.28	1.70	2.02	3.72
	S8	T	17.21	18.98	21.10	1.77	2.12	3.89
	S9	Lower	17.10	18.80	20.81	1.71	2.01	3.72
	S10		16.02	17.77	19.81	1.75	2.04	3.79

the irrigated areas to be expanded in the next decades, there is needed a public policy of incentives on improving the mobility of cropland to increase water conservation for irrigation (Fachinelli et al., 2020);

and policies for preventing water losses as well as expanding new irrigation techniques; developing alternate sources, such as rainfall harvest by small reservoirs and reuse of return flow in farming.

Annual temperature trend analysis

Table 5 shows the annual variation in average minimum temperature for different periods in two climate scenarios (RCP4.5 and RCP8.5), in the analyzed sub-regions of the São Francisco basin (Figure 2). According to the results obtained, for the RCP 4.5 scenario, there will be a tendency for minimum temperature to increase in all stations in the basin analyzed for all physiographic regions considered. However, it is clear that there will be a higher temperature level between 2060-2100 in this forcing.

In the RCP 8.5 scenario, the same trend of increased temperature remains, but with higher rates, in all regions of São Francisco, with a predicted increase of up to 3.89 °C. As with forcing 4.5, in this scenario the largest projections regarding temperature rise are predicted for the period between 2060-2100.

The observed trend of reduced precipitation in several seasons of the São Francisco River Basin contrasts with projections of increased rainfall in future decades. This discrepancy highlights the complexity of climate dynamics and regional variability.

Current reductions in precipitation may result from shortterm variability or specific climatic patterns affecting the region. These trends could be influenced by factors such as localized weather anomalies, changes in atmospheric circulation, or ongoing drought conditions.

However, long-term projections indicate a potential increase in rainfall due to broader climatic shifts, including changes in global temperature and increased moisture availability in the atmosphere. These projections account for more significant shifts in weather patterns and potential changes in the frequency and intensity of precipitation events over extended periods.

This divergence underscores the need for adaptive management strategies that consider both immediate observed conditions and longer-term projections. It also emphasizes the importance of continued monitoring and research to refine climate models and better understand the regional impacts of global climate trends.

Figure 11a, b illustrates the annual average minimum and maximum temperature over the entire São Francisco River from the perspective of the two future scenarios analyzed (RCP 4.5 and 8.5) and the current period observed. Compared to the historical period, the results showed increasing minimum and maximum temperature values in the two future scenarios, and both RCPs. Higher annual averages, both for the minimum temperature and the maximum temperature, were observed in the Lower, Medium, and Sub-Medium São Francisco.

These results corroborate those obtained comparing 27 CMIP5 models for the São Francisco River Basin (Silveira et al., 2016), all of which showed a positive trend (increase) in temperature in the period from 2011 to 2100, but more significant between 2041 and 2100. In all of them, the 8.5 scenarios showed a higher positive trend than the 4.5 RCP scenario.

Table 6 shows the annual variation in average maximum temperature for different periods in two climate scenarios (RCP4.5 and RCP8.5), in the analyzed sub-regions of the São Francisco basin (Figure 2). According to the results obtained, for the RCP 4.5 scenario, there will also be an increase in the maximum temperature in this scenario, especially for the period between 2060-2100, whose variation is 1.57 to 2.07 °C. In the RCP

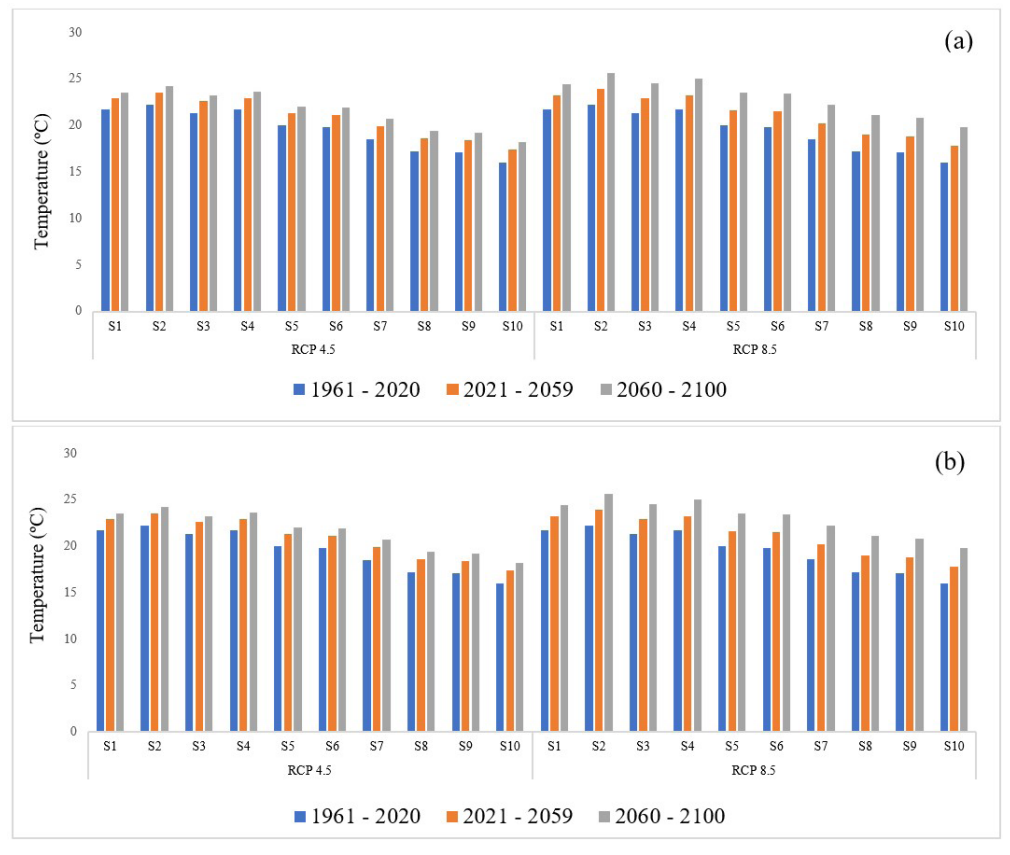


Figure 11. Mean annual minimum (a) and maximum (b) temperature (°C) for the entire São Francisco River basin.

Table 6. Variation of annua	l average maximum tempera	ture for different	periods under the Ro	CP 4.5 and RCP 8.5 scenarios.

Camaria	C4 -4:	Danian	1961 - 2020	2021 - 2059	2060 - 2100	V1	V2	V3
Scenario	Station	Region	(T1) °C	(T2) °C	(T3) °C	(T2-T1) °C	(T3-T2) °C	(T3-T1) °C
	S1	T T	31.20	32.20	32.77	1.00	0.57	1.57
	S2	Upper	33.21	34.33	34.93	1.20	0.61	1.72
	S3		32.10	33.23	33.78	1.12	0.56	1.68
	S4	MSM	32.19	33.40	33.99	1.21	0.59	1.80
RCP 4.5	S5	MSM	33.27	34.56	35.12	1.29	0.57	1.85
KCP 4.5	S6		32.61	33.89	34.42	1.27	0.53	1.80
	S7		31.56	32.89	33.46	1.33	0.57	1.90
	S8	Lower	28.18	29.60	30.26	1.42	0.65	2.07
	S9		29.46	30.86	31.51	1.40	0.65	2.04
	S10		29.67	31.03	31.65	1.36	0.62	1.97
	S1		31.20	32.43	33.74	1.23	1.31	2.54
	S2	Upper	33.22	34.60	36.01	1.38	1.40	2.79
	S3		32.12	33.50	34.74	1.38	1.24	2.62
	S4	MCM	32.20	33.69	34.94	1.49	1.24	2.73
DCD 0.5	S5	MSM	33.29	34.83	36.09	1.54	1.26	2.80
RCP 8.5	S6		32.64	34.13	35.32	1.49	1.19	2.68
	S7		31.59	33.15	34.50	1.56	1.36	2.92
	S8	T	28.21	29.90	31.42	1.70	1.52	3.22
	S9	Lower	29.48	31.14	32.73	1.66	1.59	3.25
	S10		29.69	31.29	32.90	1.59	1.61	3.20

8.5 scenario, the same trend of increased maximum temperature remains, but with higher rates, in all regions of São Francisco, with a predicted increase of up to 3.25 °C. As with forcing 4.5, in this scenario the largest projections regarding temperature rise are predicted for the period between 2060-2100, especially in the lower São Francisco region.

When compared through four (4) no-parametric trend tests used in this work, the increasing trend minimum temperature was evidenced by the Mann-Kendall Test (MK), BCPW and the Spearman correlation test shows a strong trend correlation, except for station S7 and S10, which showed a decreasing trend to minimum temperature (Figure 12). In these three tests, the results point to a higher increase in the minimum temperature in the regions of medium and upper São Francisco. The PWMK showed that the areas of Baixo São Francisco will experience a greater trend in minimum temperatures in the region.

In relation to maximum temperature, the tests proved to be more uniform in their results, except for the PWMK which presented lower values, but with a similar variation in the temperature increase trend throughout the basin (Figure 13). The Mann-Kendall (MK), BCPW and Spearman tests indicated a strong correlation and an increasing trend in the lower and upper São Francisco regions, especially in the extremities.

Monthly minimum temperature trend analysis

Figures 14-16 show the stations-wise mean monthly minimum temperature in the dry (a), rainy (b), and pre-season (c) periods, over the São Francisco River basin (Lower, Middle and Sub-Middle, and Upstream sub-regions).

For the Lower São Francisco (Figure 14a-c), the stationwise mean monthly minimum temperature will increase over the two future periods, when compared to the historical observed period, in both future RCPs.

For the Middle and Sub-Middle São Francisco (Figure 15a-c), the obtained results compared to the observed period, the monthly average of the minimum temperature will increase over the two future periods, gradually, in all stations in the sub-regions analyzed, regardless of the RCP to be considered.

The same behavior is projected for the Upper São Francisco (Figure 16a-c), whose minimum temperature will also increase gradually, for the two scenarios analyzed, and in all seasons analyzed.

Monthly maximum temperature trend analysis

Figure 17a-c, presents a station-wise mean maximum temperature (°C) analysis over Lower São Francisco, showing an increasing average monthly maximum temperature in the two future periods under the RCP 4.5 and RCP 8.5 scenarios if compared to the historical observed period. Behavior similar to that of the minimum temperature for this region, however with higher values.

Figure 18a-c shows an analysis of average maximum temperature (°C) per station in the Middle and Sub middle São Francisco. Just like in the lower São Francisco, in this region there will also be an increase in the maximum temperature in the future periods analyzed under the RCP 4.5 and RCP 8.5 scenarios, whose temperature could reach 38 °C in the pre-season period, reaching a variation of 4° in relation to the data observed today and 2nd in relation to the least pessimistic scenario (RCP 4.5) (Figure 18c).

Figure 19a-c shows an analysis of average maximum temperature (°C) per station in the Upper São Francisco. Just like in the lower and Middle and Sub-Middle São Francisco, in this region there will also be an increase in the maximum temperature in the future periods analyzed under the RCP 4.5 and RCP 8.5 scenarios, whose temperature could vary from 30 to 35 °C, especially in the

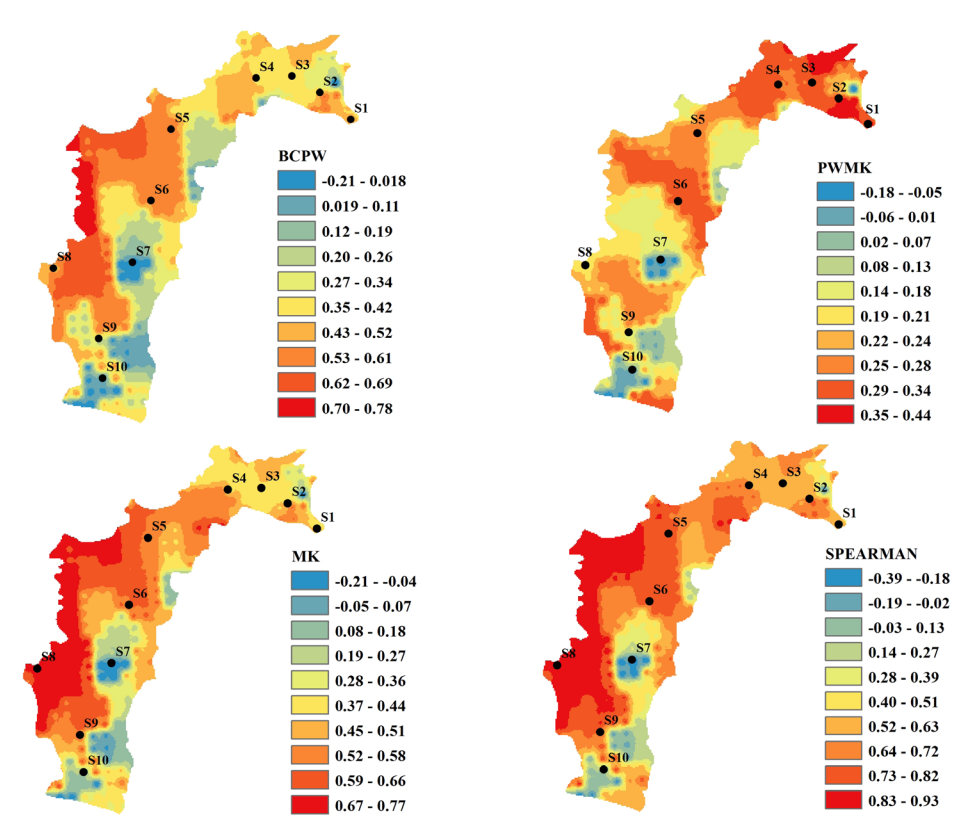


Figure 12. Spatial variation of Z-value and trend showing grid points in four trend tests of minimum temperature data annual period over the São Francisco River Basin.

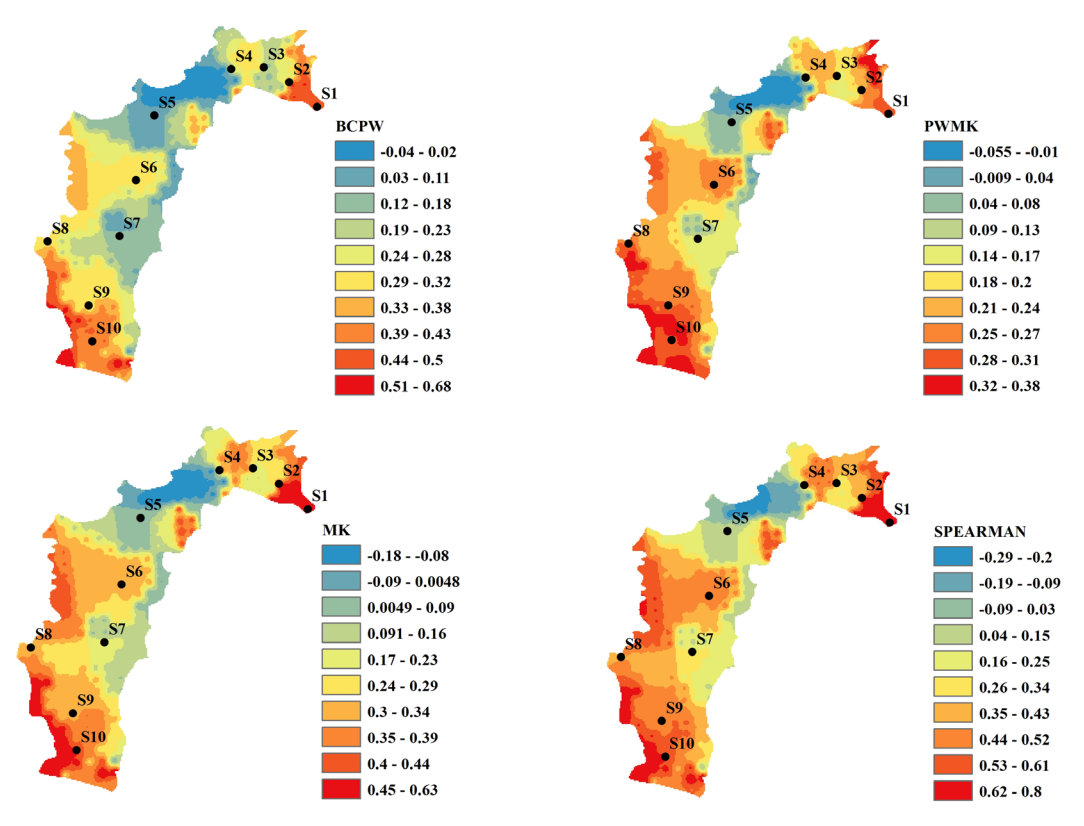


Figure 13. Spatial variation of Z-value and trend showing grid points in four trend tests of maximum temperature data annual period over the São Francisco River Basin.

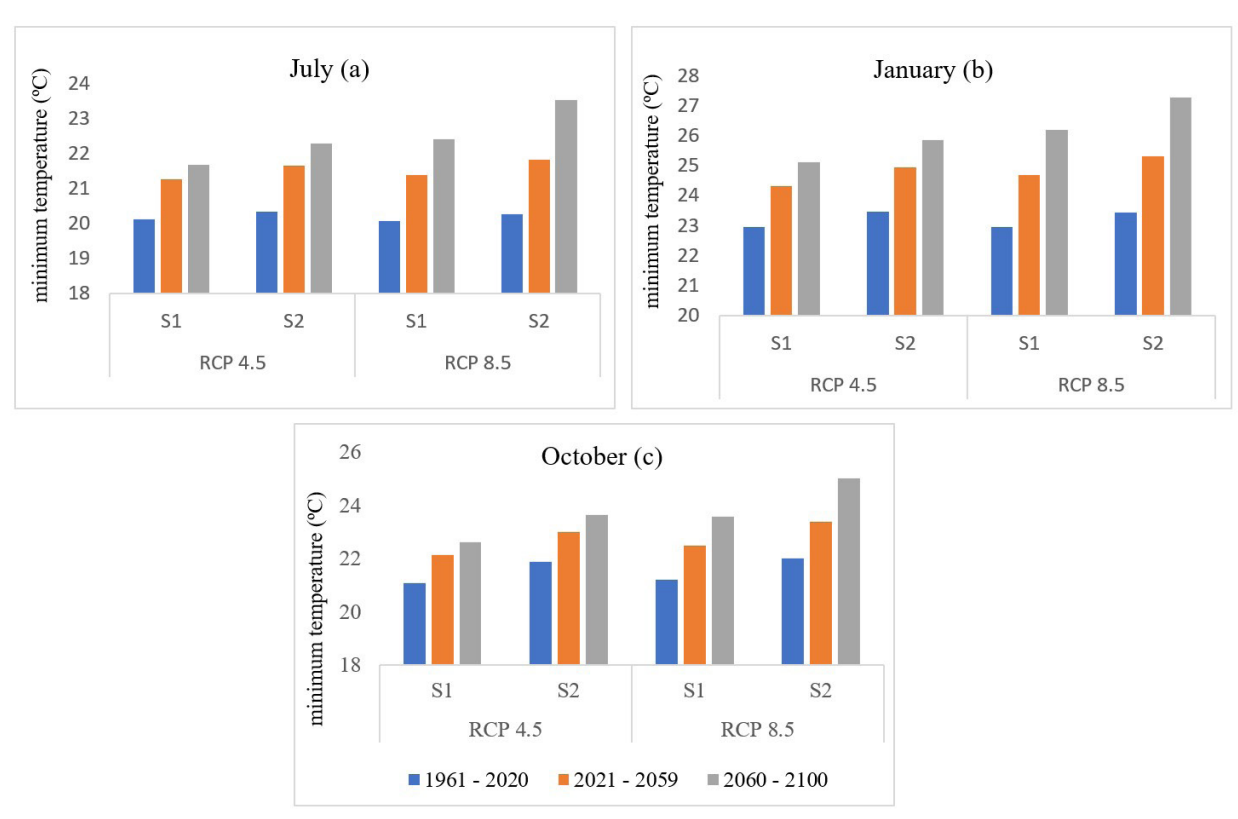


Figure 14. Station-wise mean monthly minimum temperature (°C) in the dry (a), rainy (b), and pre-season (c) periods over Lower São Francisco.

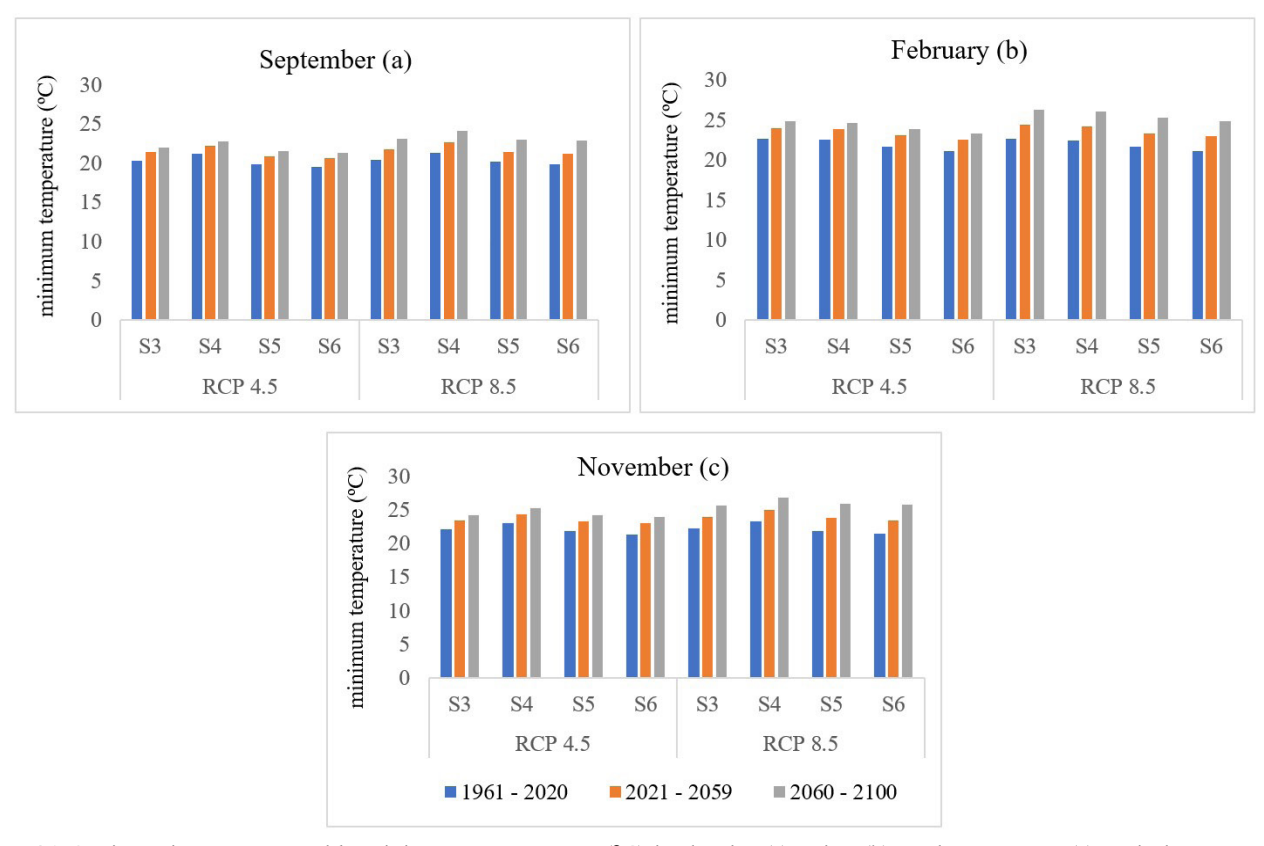


Figure 15. Station-wise mean monthly minimum temperature (°C) in the dry (a), rainy (b), and pre-season (c) periods over Middle and Sub-Middle São Francisco.

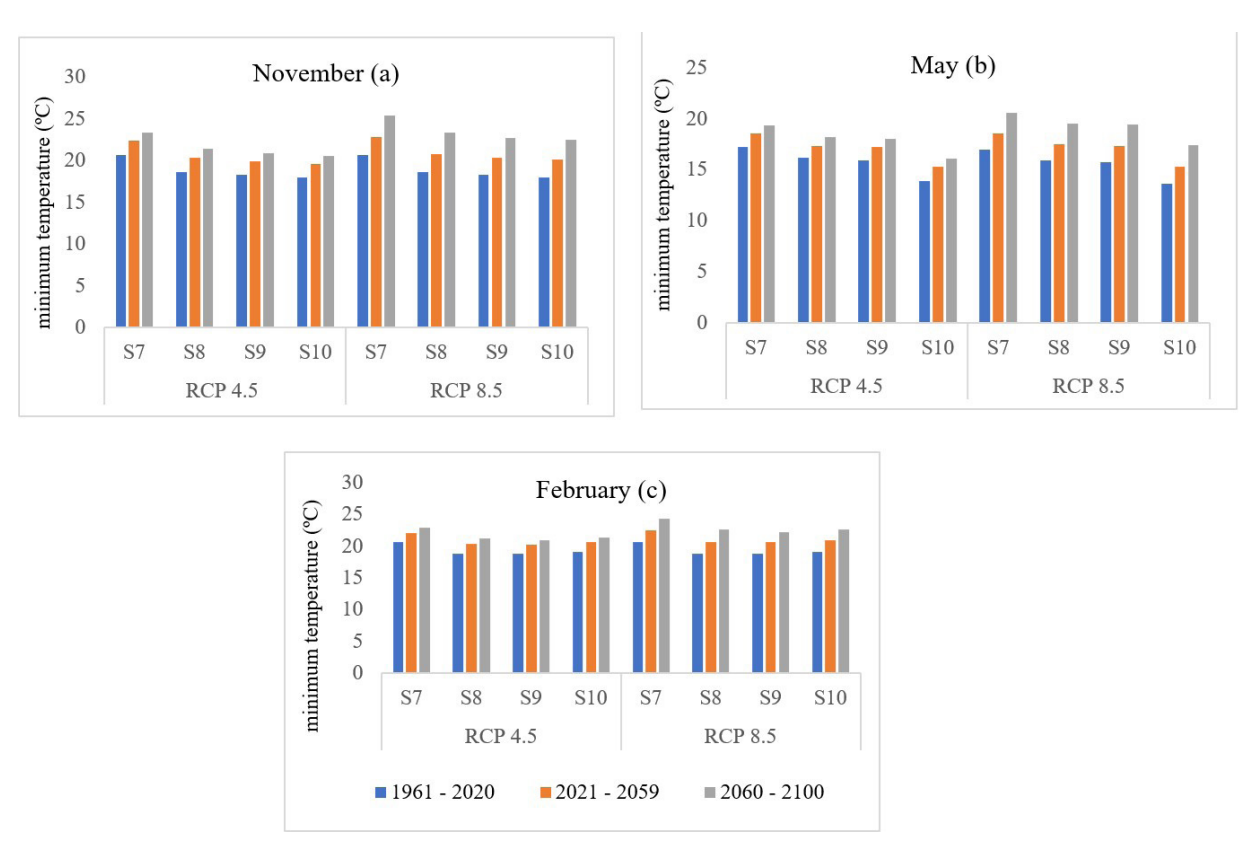


Figure 16. Station-wise mean monthly minimum temperature (°C) in the dry (a), rainy (b), and pre-season (c) periods over Upper São Francisco.

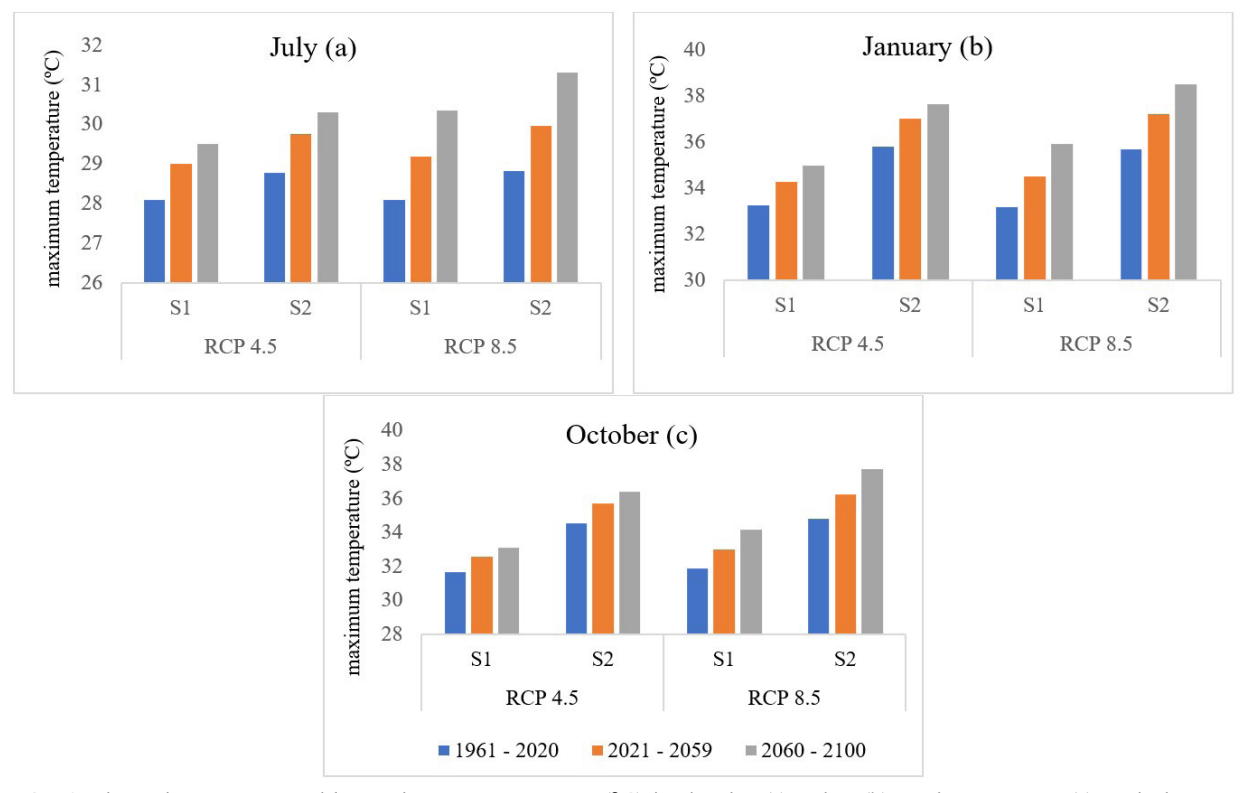


Figure 17. Station-wise mean monthly maximum temperature (°C) in the dry (a), rainy (b), and pre-season (c) periods over Lower São Francisco.

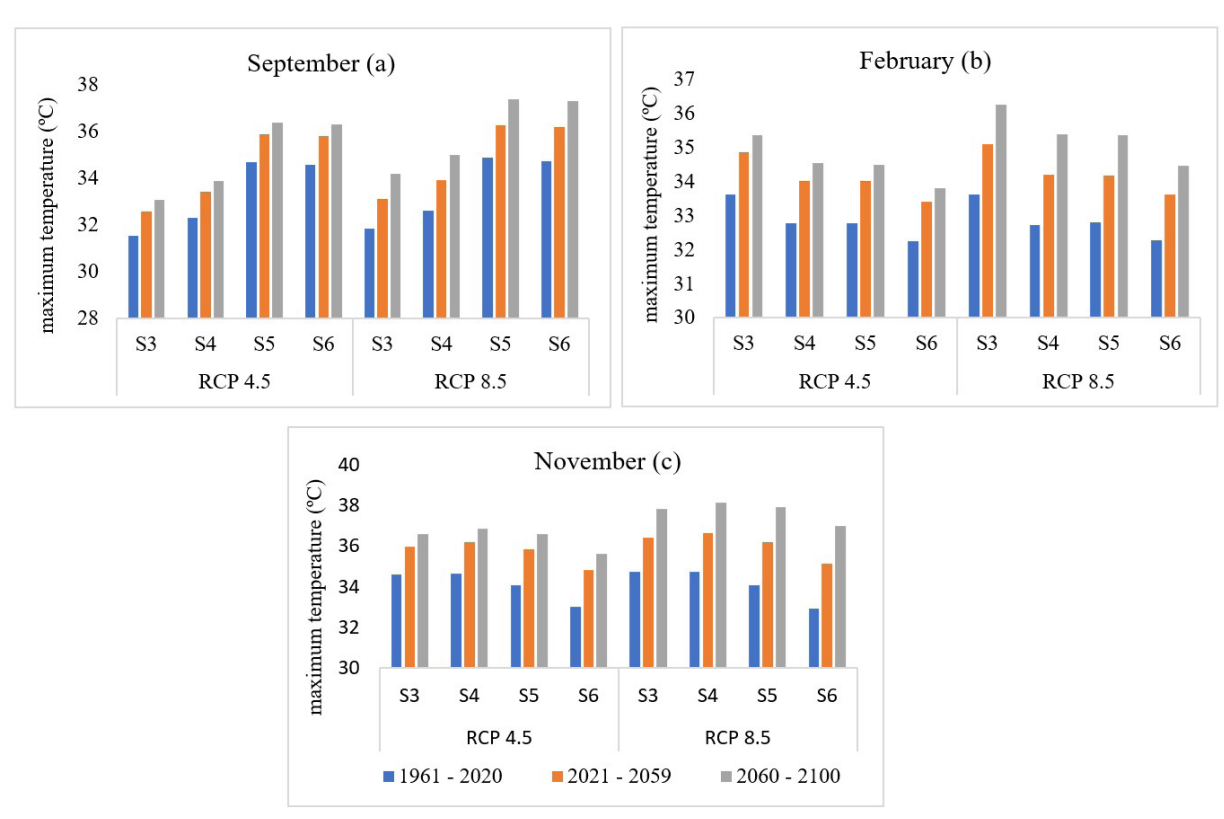


Figure 18. Station-wise mean monthly maximum temperature (°C) in the dry (a), rainy (b), and pre-season (c) periods over Middle and Sub-Middle São Francisco.

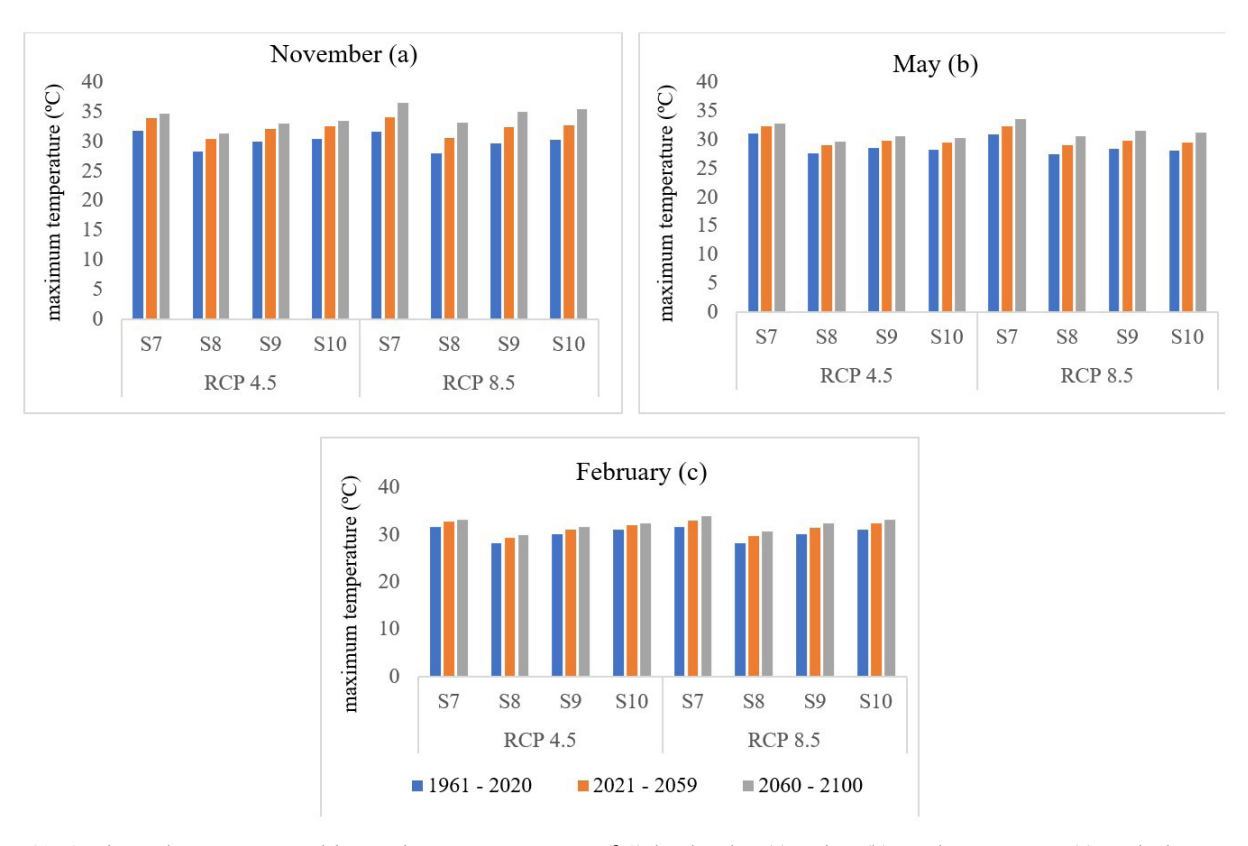


Figure 19. Station-wise mean monthly maximum temperature (°C) in the dry (a), rainy (b), and pre-season (c) periods over Upper São Francisco.

dry period (Figure 19a). The RCP8.5 scenario, as in other analyses, presents higher estimates for the increase in maximum temperature in the basin, with a forecast increase of 1 to 2 degrees in relation to the observed period and the RCP 4.5 scenario.

These results corroborate with the ones found by Silva & Azevedo (2012), that evaluating climate change detention indices for the Bahia State between 1970 and 2006 and diagnosed that the number of days with daily maximum temperature increased, while the daily rainfall and total annual precipitation reduced. Also, a faster increase of daily temperature due to the climate change scenarios for 2010-2050, over the Northeastern of the Munneru basin, India, compared to that simulated for the recent past was reported (Buri et al., 2022), indicating possible aridization process.

DISCUSSION

The results of the uncertainty analyses, in their different methods, in the precipitation and temperature data sets addressed in this research for the São Francisco River basin indicated variability throughout the studied period, both in time and space, when taking into account the heterogeneity of the basin. The analyses regarding the trend of annual precipitation in the ten areas analyzed in the basin, for the two scenarios emissions (RCP 4.5 and 8.5), in general, indicate that there will be a slight increase in precipitation in the basin for the periods analyzed, however, scenario 8.5 predicts lower rainfall rates when compared to 4.5. Non-parametric tests indicated higher trends in the Middle, Upper and Sub-Middle São Francisco regions. Similar agreement of a possible scenario increasing in magnitude and frequency of extreme precipitation, was found with rainfall changes in various parts of South America by 2070-2100 (Manatsa et al., 2008; Marengo et al., 2010; Bezerra et al., 2019), using different regional models, as well as the projected changes of rainfall from the IPCC AR4 multi-model ensemble for the same scenarios, and the rainfall projections derived from Eta-CPTEC by the end of the 21st-century, showing increases in rainfall in southeastern South America (Marengo et al., 2012).

When the results are analyzed by seasons and by physiographic area of the basin (dry, rainy and pre-season), the trends follow the peculiarities and climatic characteristics of each region. In the lower São Francisco, the projections indicate a decrease in rainfall in the pre-season and dry season, and a slight increase in the rainy season. Similar trends were also estimated in the Middle and Sub-Middle São Francisco, where the projections decrease in the pre-season and dry season and show a slight increase in the rainy season. This is different from the Upper region, which projects a decrease in rainfall in both the dry and rainy seasons, and higher rates in the pre-season, in both forcing factors addressed.

These results are consistent with the historical phenomenon of rainfall deficit registered during the dry summer of 2001, which reached up to 40% in most of central, northeastern, and southeastern Brazil, resulting in a significant reduction in river streamflow throughout this regions, thereby reducing the capacity to produce hydroelectric power in these areas, and compromising the amount of water available along the basin (Freitas et al., 2022). The alignment of these results can also be verified in the consequence of the multiyear drought, for the period 2014-2019 observed rainfall in the São Francisco basin reported in

the past (de Jong et al., 2021), was 37% below if compared to its 1961-1990 baseline average and, consequently, observed streamflow declined by approximately 60%.

Further, the São Francisco River basins' streamflow and hydroelectric production could potentially cease in the second half of the 21st century (de Jong et al., 2021). Therefore, to face the upcoming scenarios of climate change, impositions of energy conservation measures from the government side will be required to avoid total loss of power (blackouts), as well as the reconfiguration in the NE electrical matrix shortly, considering economic, technical and social environmental constraints (Souza Júnior et al., 2021). Alternatively, the design of PV-hydro hybrid systems (based on complementary resources) for providing energy (Vasco et al., 2019), can be explored as an effective strategy to cope with future climate change scenarios, and supply water for irrigation (among other uses) as the major component of water demand accounted for 67% of the total demand (Teixeira et al., 2021). All of this variation in precipitation in the region is due to large-scale circulation, whereas the rainfall intensity may be influenced by climate variability (Assis et al., 2022).

Regarding the maximum and minimum temperature projections for the basin, the results indicate an increase in them in all the physiographic regions analyzed and, in the stations, covered, as well as in their different periods, both annual and monthly. According to the projections, RCP 8.5 indicates higher temperatures when compared to 4.5. In both forcing 4.5 and 8.5, the period of greatest temperature increase in the basin will occur between 2060 and 2100. The non-parametric tests analyzed also indicate an increase in the minimum and maximum temperature in the different regions of the basin, with better adjustments in the Mann-Kendall (MK), BCPW and Spearman tests.

According to Marengo (2014) and Reboita et al. (2018), the temperature will tend to increase throughout the SF basin, and in some areas of the basin it may reach up to 5 °C. According to the authors, extreme heat and precipitation are also expected in these projections, as well as longer periods of drought. According to Silveira et al. (2016), the temperature will increase in the São Francisco basin by 2 °C in the RCP 4.5 scenario and by over 4 °C in 8.5, between 2011 and 2100. According to the climate projections analyzed by the authors, addressing the CMIP5 models, there will be an increase in the water deficit, a reduction in the flow in the basin and, consequently, a reduction in the annual average energy produced by hydroelectric plants in the SFRB. de Jong et al. (2018) indicates that these projections for the SF region could make it an area more susceptible to more severe droughts.

CONCLUSIONS

This study analyzes long-term trends in precipitation and temperature data sets (maximum and minimum values) projected by NEX-GDDP in the São Francisco River Basin under RCP 4.5 and RCP 8.5 scenarios.

In the analysis of precipitation metrics, the results for the NRMSD showed that, in general, the CSIRO model presented more satisfactory results in all physiographic regions. For temperature, the analysis of this metric also showed good results among the models for the stations analyzed. Person's correlation coefficient

showed a better adjustment of precipitation for the MIROC5, EC.EARTH and NORESMI1 models, in areas of sub-medium and upper São Francisco. For the minimum temperature, the CSIRO and NORESMI1 models showed the best fit, in general. At maximum temperature, the EC.EARTH and CSIRO models showed more satisfactory results.

Regarding the annual precipitation trend in the basin, the results indicated, in general, considering the stations analyzed, that there will be an increase in rainfall until 2100 for both scenarios analyzed (RCP 4.5 and 8.5). However, scenario 8.5 indicates higher rainfall rates than scenario 4.5, in all regions analyzed, with variations between stations. The increasing trend of precipitation when evaluated through four non-parametric trend tests showed an increasing trend in the Upper, Medium, and Sub-medium São Francisco. About the monthly average precipitation by physiographic regions, the results indicated some variations between the stations located in these areas. In Lower São Francisco, projections indicate different behavior for the periods analyzed in both scenarios, with an increase in rainfall in the rainy season and a decrease in rainfall in the dry and pre-season. This also occurs in the region of medium and sub-medium São Francisco, with a decrease in rainfall in the dry and pre-season and an increase in the rainy season. In Alto SF, projections indicate a decrease in rainfall in the dry and rainy season and an increase in the pre-season.

For annual temperature, the results show an increase in both the minimum and maximum temperatures throughout the basin, in the two RCP scenarios analyzed. With regard to monthly averages, the results for minimum and maximum temperatures indicate, in general, also an increase for the three periods analyzed, in the two scenarios adopted, especially between 2060 and 2100.

In the context of climate change, the uncertainties associated with RCMs and scenarios need to be assessed in order to implement effective management practices and make informed decisions. The results are used as input to hydrological and water resource management models under climate change scenarios.

ACKNOWLEDGEMENTS

This study was supported by the Coordenação de Aperfeiçoamento de Pessoal de Nível Superior - CAPES, through the doctoral fellowship of the first author and the National Council for Scientific and Technological Development – CNPq, through the third author's visiting expert (EV1) grant (Proc. 383745/2022-5), by the Universal Announcement Project (431980/2018-7), BRICS project (442335/2017-2), INCT - National Observatory for Water Security and Adaptive Management (Proc. 406919/2022-4) and the ninth author's Productivity and Research grant (313392/2020-0).

REFERENCES

Achite, M., Ceribasi, G., Ceyhunlu, A. I., Walega, A., & Caloiero, T. (2021). The Innovative Polygon Trend Analysis (IPTA) as a simple qualitative method to detect changes in environment: example detecting trends of the total monthly precipitation in semiarid area. *Sustainability*, *13*(22), 12674. http://doi.org/10.3390/su132212674.

Achite, M., Ceribasi, G., Wałęga, A., Ceyhunlu, A. I., Elshaboury, N., Krakauer, N., Hartani, T., Caloiero, T., & Gul, S. (2023). Analysis of monthly average precipitation of Wadi Ouahrane basin in Algeria by using the ITRA, ITPAM, and TPS methods. *Environmental Monitoring and Assessment*, 195(5), 606. http://doi.org/10.1007/s10661-023-11236-3.

Agência Nacional de Águas e Saneamento Básico – ANA. (2024). Retrieved in 2024, May 11, from https://www.snirh.gov.br/hidroweb/serieshistoricas

Agência Pernambucana de Águas e Clima – APAC. (2024). *Monitoramento*. Retrieved in 2024, May 11, from https://www.apac.pe.gov.br/monitoramento

Ahmed, K., Sachindra, D. A., Shahid, S., Iqbal, Z., Nawaz, N., & Khan, N. (2020). Multi-model ensemble predictions of precipitation and temperature using machine learning algorithms. *Atmospheric Research*, 236, 104806. http://doi.org/10.1016/j.atmosres.2019.104806.

Ahmed, N., Wang, G., Booij, M. J., Ceribasi, G., Bhat, M. S., Ceyhunlu, A. I., & Ahmed, A. (2022). Changes in monthly streamflow in the Hindukush-Karakoram-Himalaya Region of Pakistan using innovative polygon trend analysis. *Stochastic Environmental Research and Risk Assessment*, 36(3), 811-830. http://doi.org/10.1007/s00477-021-02067-0.

Andrade, C. W. L., Montenegro, S. M. G. L., Montenegro, A. A. A., Lima, J. R. S., Srinivasan, R., & Jones, C. A. (2021). Climate change impact assessment on water resources under RCP scenarios: a case study in Mundaú River Basin, Northeastern Brazil. *International Journal of Climatology*, 41(S1), E1045-E1061. http://doi.org/10.1002/joc.6751.

Andreoli, R. V., & Kayano, M. T. (2005). ENSO-related rainfall anomalies in South America and associated circulation features during warm and cold Pacific decadal oscillation regimes. *International Journal of Climatology*, *25*(15), 2017-2030. http://doi.org/10.1002/joc.1222.

Assis, J. M. O., Caldas, H. F. M., Sobral, M. C. M., Souza, W. M., & Melo, M. G. S. (2022). Analysis of climate indices and impacts on the rainfall regime in the Submedium region of the São Francisco river basin – Brazil. *Revista Principia*, *59*(4), 1475-1486. http://doi.org/10.18265/1517-0306a2021id5570.

Assis, J. M. O., Souza, W. M., & Sobral, M. (2015). Análise climática da precipitação no submédio da bacia do Rio São Francisco com base no índice de anomalia de chuva. Revista Brasileira de Ciências Ambientais, (36), 115-127. http://doi.org/10.5327/Z2176-947820151012.

Banerjee, A., Chen, R. E., Meadows, M., Singh, R. B., Mal, S., & Sengupta, D. (2020). analysis of long-term rainfall trends and variability in the Uttarakhand Himalaya using Google Earth engine. *Remote Sensing*, 12(4), 709. http://doi.org/10.3390/rs12040709.

Bartier, P. M., & Keller, C. P. (1996). Multivariate interpolation to incorporate thematic surface data using Inverse Distance Weighting (IDW). *Computers & Geosciences*, 22(7), 795-799. http://doi.org/10.1016/0098-3004(96)00021-0.

Bezerra, B. G., Silva, L. L., Santos, C. M. S., & Carvalho, G. G. (2019). Changes of precipitation extremes indices in São Francisco River Basin, Brazil from 1947 to 2012. *Theoretical and Applied Climatology*, 135(1–2), 565-576. http://doi.org/10.1007/s00704-018-2396-6.

Biswas, R. N., Islam, M. N., Mia, M. J., & Islam, M. N. (2020). Modeling on the spatial vulnerability of lightning disaster in Bangladesh using GIS and IDW techniques. *Spatial Information Research*, 28(5), 507-521. http://doi.org/10.1007/s41324-019-00311-y.

Brasil. Ministério da Ciência, Tecnologia e Inovação – MCTI. (2013). Sumário executivo: base científica das mudanças climáticas: contribuição do grupo de trabalho 1 ao primeiro relatório de avaliação nacional do Painel Brasileiro de Mudanças Climáticas (PBMC). Brasília: MCTI.

Buri, E. S., Keesara, V. R., Loukika, K. N., & Sridhar, V. (2022). Spatio-temporal analysis of climatic variables in the Munneru River basin, India, using NEX-GDDP data and the REA approach. *Sustainability*, *14*(3), 1715. http://doi.org/10.3390/su14031715.

Carvalho, A. A., Montenegro, A. A. A., Silva, H. P., Lopes, I., Morais, J. E. F., & Silva, T. G. F. (2020). Trends of rainfall and temperature in Northeast Brazil Tendências da precipitação pluvial e da temperatura no Nordeste brasileiro. Revista Brasileira de Engenharia Agrícola e Ambiental, 24(1), 15-23. http://doi.org/10.1590/1807-1929/agriambi.v24n1p15-23.

Clark, M. P., Wilby, R. L., Gutmann, E. D., Vano, J. A., Gangopadhyay, S., Wood, A. W., Fowler, H. J., Prudhomme, C., Arnold, J. R., & Brekke, L. D. (2016). Characterizing uncertainty of the hydrologic impacts of climate change. *Current Climate Change Reports*, *2*(2), 55-64. http://doi.org/10.1007/s40641-016-0034-x.

de Jong, P., Barreto, T. B., Tanajura, C. A. S., Oliveira-Esquerre, K. P., Kiperstok, A., & Andrade Torres, E. (2021). The impact of regional climate change on hydroelectric resources in South America. *Renewable Energy*, 173, 76-91. http://doi.org/10.1016/j.renene.2021.03.077.

de Jong, P., Tanajura, C. A. S., Sánchez, A. S., Dargaville, R., Kiperstok, A., & Torres, E. A. (2018). Hydroelectric production from Brazil's São Francisco River could cease due to climate change and inter-annual variability. *The Science of the Total Environment*, 634, 1540-1553. http://doi.org/10.1016/j.scitotenv.2018.03.256.

Edwards, A. W. F., & Cavalli Sforza, L. L. (1965). A method for cluster analysis. *Biometrics*, 21(2), 362-375. http://doi.org/10.2307/2528096.

Fachinelli, F. A. S., Ferreira Filho, J. B. S., Cuadra, S. V., & Victoria, D. C. (2020). Water demand prospects for irrigation in the são francisco river: brazilian public policy. *Water Policy*, 22(3), 449-467. http://doi.org/10.2166/wp.2020.215.

Ferreira, D. B., Barroso, G. R., Dantas, M. S., Oliveira, K. L., Christofaro, C., & Oliveira, S. C. (2021). Pluviometric patterns in the São Francisco River basin in Minas Gerais, Brazil. *RBRH*, *26*, e27. http://doi.org/10.1590/2318-0331.262120210035.

Fonseca, M. G., Alves, L. M., Aguiar, A. P. D., Arai, E., Anderson, L. O., Rosan, T. M., Shimabukuro, Y. E., & Aragão, L. E. O. C. (2019). Effects of climate and land-use change scenarios on fire probability during the 21st century in the Brazilian Amazon. *Global Change Biology*, 25(9), 2931-2946. http://doi.org/10.1111/gcb.14709.

Freitas, A. A., Drumond, A., Carvalho, V. S. B., Reboita, M. S., Silva, B. C., & Uvo, C. B. (2022). Drought Assessment in São Francisco River Basin, Brazil: characterization through SPI and Associated Anomalous Climate Patterns. *Atmosphere*, *13*(1), 41. http://doi.org/10.3390/atmos13010041.

Galvíncio, J. D. (2000). *Impactos dos eventos el nino na precipitação da bacia do rio São Francisco* (Dissertação de mestrado). Universidade Federal da Paraíba, Campina Grande.

Gebrechorkos, S. H., Hülsmann, S., & Bernhofer, C. (2019). Changes in temperature and precipitation extremes in Ethiopia, Kenya, and Tanzania. *International Journal of Climatology*, 39(1), 18-30. http://doi.org/10.1002/joc.5777.

Hundecha, Y., & Bárdossy, A. (2005). Trends in daily precipitation and temperature extremes across western Germany in the second half of the 20th century. *International Journal of Climatology*, 25(9), 1189-1202. http://doi.org/10.1002/joc.1182.

Hussain, F., Ceribasi, G., Ceyhunlu, A. I., Wu, R.-S., Cheema, M. J. M., Noor, R. S., Anjum, M. N., Azam, M., & Afzal, A. (2022). Analysis of precipitation data using innovative trend pivot analysis method and trend polygon star concept: a case study of Soan River Basin, Potohar Pakistan. *Journal of Applied Meteorology and Climatology*, 61(12), 1861-1880. http://doi.org/10.1175/JAMC-D-22-0081.1.

Instituto Nacional de Meteorologia – INMET. (2024). Retrieved in 2024, May 11, from http://www.inmet.gov.br/projetos/rede/pesquisa/inicio.php

Isotta, F. A., Begert, M., & Frei, C. (2019). Long-term consistent monthly temperature and precipitation grid data sets for switzerland over the past 150 years. *Journal of Geophysical Research. Atmospheres*, 124(7), 3783-3799. http://doi.org/10.1029/2018JD029910.

Kanda, N., Negi, H. S., Rishi, M. S., & Kumar, A. (2020). Performance of various gridded temperature and precipitation datasets over northwest himalayan region. *Environmental Research Communications*, *2*(8), 085002. http://doi.org/10.1088/2515-7620/ab9991.

Kotir, J. H. (2011). Climate change and variability in Sub-Saharan Africa: a review of current and future trends and impacts on agriculture and food security. *Environment, Development and Sustainability*, 13(3), 587-605. http://doi.org/10.1007/s10668-010-9278-0.

Li, Y., Qin, X., Liu, Y., Jin, Z., Liu, J., Wang, L., & Chen, J. (2022). Evaluation of Long-term and high-resolution gridded precipitation and temperature products in the Qilian Mountains, Qinghai-Tibet Plateau. *Frontiers in Environmental Science*, 10, 906821. http://doi.org/10.3389/fenvs.2022.906821.

Liu, J., Yang, H., Gosling, S. N., Kummu, M., Flörke, M., Pfister, S., Hanasaki, N., Wada, Y., Zhang, X., Zheng, C., Alcamo, J., & Oki, T. (2017). Water scarcity assessments in the past, present, and future. *Earth's Future*, *5*(6), 545-559. http://doi.org/10.1002/2016EF000518.

Lucas, M. C., Kublik, N., Rodrigues, D. B. B., Meira Neto, A. A., Almagro, A., Melo, D. C. D., Zipper, S. C., & Oliveira, P. T. S. (2021). Significant baseflow reduction in the sao francisco river basin. *Water*, *13*(1), 2. http://doi.org/10.3390/w13010002.

Mallakpour, I., Sadeghi, M., Mosaffa, H., Akbari Asanjan, A., Sadegh, M., Nguyen, P., Sorooshian, S., & AghaKouchak, A. (2022). Discrepancies in changes in precipitation characteristics over the contiguous United States based on six daily gridded precipitation datasets. *Weather and Climate Extremes*, *36*, 100433. http://doi.org/10.1016/j.wace.2022.100433.

Manatsa, D., Chingombe, W., & Matarira, C. H. (2008). The impact of the positive Indian Ocean dipole on Zimbabwe droughts Tropical climate is understood to be dominated by. *International Journal of Climatology*, 20(15), 2011-2029. http://doi.org/10.1002/joc.1695.

Marengo, J. A. (2014). O futuro clima do Brasil. *Revista USP*, *103*(103), 25-32. http://doi.org/10.11606/issn.2316-9036.v0i103p25-32.

Marengo, J. A., Ambrizzi, T., Rocha, R. P., Alves, L. M., Cuadra, S. V., Valverde, M. C., Torres, R. R., Santos, D. C., & Ferraz, S. E. T. (2010). Future change of climate in South America in the late twenty-first century: intercomparison of scenarios from three regional climate models. *Climate Dynamics*, *35*(6), 1073-1097. http://doi.org/10.1007/s00382-009-0721-6.

Marengo, J. A., Chou, S. C., Kay, G., Alves, L. M., Pesquero, J. F., Soares, W. R., Santos, D. C., Lyra, A. A., Sueiro, G., Betts, R., Chagas, D. J., Gomes, J. L., Bustamante, J. F., & Tavares, P. (2012). Development of regional future climate change scenarios in South America using the Eta CPTEC/HadCM3 climate change projections: climatology and regional analyses for the Amazon, São Francisco and the Paraná River basins. *Climate Dynamics*, 38(9-10), 1829-1848. http://doi.org/10.1007/s00382-011-1155-5.

Marques, E. T., Gunkel, G., & Sobral, M. C. (2019). Management of tropical river basins and reservoirs under water stress: experiences from northeast Brazil. *Environments*, 6(6), 62.

Moncunill, D. F. (2006). The rainfall trend over Ceara and its implications. In *Proceedings of 8th ICSHMO* (pp. 315-323). São José dos Campos: INPE.

Montenegro, S., & Ragab, R. (2012). Impact of possible climate and land use changes in the semi arid regions: A case study from

North Eastern Brazil. *Journal of Hydrology*, *434-435*, 55-68. http://doi.org/10.1016/j.jhydrol.2012.02.036.

Morais, D. C., & Almeida, A. T. (2012). Group decision making on water resources based on analysis of individual rankings. *Omega*, 40(1), 42-52. http://doi.org/10.1016/j.omega.2011.03.005.

Nascimento do Vasco, A., Aguiar Netto, A. O., & Silva, M. G. (2019). The influence of dams on ecohydrological conditions in the São Francisco River Basin, Brazil. *Ecohydrology & Hydrobiology*, 19(4), 556-565. http://doi.org/10.1016/j.ecohyd.2019.03.004.

Oliveira, P. T., Santos e Silva, C. M., & Lima, K. C. (2017). Climatology and trend analysis of extreme precipitation in subregions of Northeast Brazil. *Theoretical and Applied Climatology*, *130*(1-2), 77-90. http://doi.org/10.1007/s00704-016-1865-z.

Panda, A., & Sahu, N. (2019). Trend analysis of seasonal rainfall and temperature pattern in Kalahandi, Bolangir and Koraput districts of Odisha, India. *Atmospheric Science Letters*, 20(10), e932. http://doi.org/10.1002/asl.932.

Patakamuri, S. K., Muthiah, K., & Sridhar, V. (2020). Long-term homogeneity, trend, and change-point analysis of rainfall in the arid district of ananthapuramu, Andhra Pradesh State, India. *Water*, 12(1), 211. http://doi.org/10.3390/w12010211.

R Core Team. (2024). R: a language and environment for statistical computing. Vienna: R Foundation for Statistical Computing. Retrieved in 2013, August 15, from https://cran.r-project.org/web/packages/modifiedmk/index.html

Rathjens, H., Bieger, K., Srinivasan, R., Chaubey, I., & Arnold, J. G. (2016). *CMhyd user manual documentation for preparing simulated climate change data for hydrologic impact studies* (16 p.). College Station: Texas A&M University.

Reboita, M. S., Gan, M. A., Rocha, R. P., & Ambrizzi, T. (2010). Regimes de precipitação na América do Sul: uma revisão bibliográfica. *Revista Brasileira de Meteorologia*, 25(2), 185-204. http://doi.org/10.1590/S0102-77862010000200004.

Reboita, M. S., Marrafon, V. H. A., Llopart, M., & Rocha, R. P. (2018). Cenários de mudanças climáticas projetados para o estado de Minas Gerais. *Rev. Bras. Climatol.*, *1*, 110-128. http://doi.org/10.5380/abclima.v1i0.60524.

Ribeiro Neto, A., Paz, A. R., Marengo, J. A., & Chou, S. C. (2016). Hydrological processes and climate change in hydrographic regions of Brazil. *Journal of Water Resource and Protection*, 8(12), 1103-1127.

Sales, D. C., Costa, A. A., Silva, E. M., Vasconcelos Júnior, F. C., Cavalcante, A. M. B., Medeiros, S. S., Marin, A. M. P., Guimarães, S. O., Araújo Junior, L. M., & Pereira, J. M. R. (2015). Projeções de mudanças na precipitação e temperatura no nordeste Brasileiro utilizando a técnica de downscaling dinâmico. *Revista Brasileira de Meteorologia*, 30(4), 435-456. http://doi.org/10.1590/0102-778620140075.

Santos, T. V., Freitas, L. A., Gonçalves, R. D., & Chang, H. K. (2020). Teste de Mann-Kendall aplicado à dados hidrológicos: desempenho dos filtros TFPW e CV2 na análise de tendências. *Ciência e Natura*, 42, e87. http://doi.org/10.5902/2179460X41928.

Sarioz, I. O., Ceribasi, G., & Ceyhunlu, A. I. (2024). Investigation of the variability applying classical (MK-SR) and modern (ITTA-TPSC) trend methods to meteorological parameters of Marmara Basin in Turkey. *Physics and Chemistry of the Earth Parts A/B/C*, 135, 103665. http://doi.org/10.1016/j.pce.2024.103665.

Schwalm, C. R., Glendon, S., & Duffy, P. B. (2020). RCP8.5 tracks cumulative CO2 emissions. *Proceedings of the National Academy of Sciences of the United States of America*, 117(33), 19656-19657. http://doi.org/10.1073/pnas.2007117117.

Silva, G. B., & Azevedo, P. V. (2012). Cenários de mudanças climáticas no estado da Bahia através de estudos numéricos e estatísticos. *Revista de Geografia Fisica*, 5, 1019-1034.

Silveira, C. S., Souza Filho, F. A., Martins, E. S. P. R., Oliveira, J. L., Costa, A. C., Nobrega, M. T., Souza, S. A., & Silva, R. F. V. (2016). Mudanças climáticas na bacia do rio São Francisco: uma análise para precipitação e temperatura. *RBRH*, *21*(2), 416-428. http://doi.org/10.21168/rbrh.v21n2.p416-428.

Siqueira, N. A. S., Siqueira, A. H. B., & Pereira Filho, A. J. (2022). Statistical analysis of precipitation extremes in São Francisco River Basin, Brazil *Atmospheric and Climate Science*, *12*(2), 383-408. http://doi.org/10.4236/acs.2022.122023.

Souto, J., Beltrão, N., & Teodoro, A. (2019). Performance of remotely sensed soil moisture for temporal and spatial analysis of rainfall over São Francisco River basin, Brazil. *Geosciences*, 9(3), 144. http://doi.org/10.3390/geosciences9030144.

Souza Júnior, C. B., Koch, H., Siegmund-Schultze, M., & Köppel, J. (2021). An exploratory scenario analysis of strategic pathways towards a sustainable electricity system of the drought-stricken São Francisco River Basin. *Energy Systems*, 12(3), 563-602. http://doi.org/10.1007/s12667-019-00343-1.

Teixeira, A. L. F., Bhaduri, A., Bunn, S. E., & Ayrimoraes, S. R. (2021). Operationalizing water security concept in water investment planning: case study of São Francisco river basin. *Water*, *13*(24), 3658. http://doi.org/10.3390/w13243658.

Teutschbein, C., & Seibert, J. (2012). Bias correction of regional climate model simulations for hydrological climate-change impact studies: review and evaluation of different methods. *Journal of Hydrology*, 456-457, 12-29. http://doi.org/10.1016/j.jhydrol.2012.05.052.

Teutschbein, C., & Seibert, J. (2013). Is bias correction of regional climate model (RCM) simulations possible for non-stationary

conditions. *Hydrology and Earth System Sciences*, *17*(12), 5061-5077. http://doi.org/10.5194/hess-17-5061-2013.

Thomson, A. M., Calvin, K. V., Smith, S. J., Kyle, G. P., Volke, A., Patel, P., Delgado-Arias, S., Bond-Lamberty, B., Wise, M. A., Clarke, L. E., & Edmonds, J. A. (2011). RCP4.5: a pathway for stabilization of radiative forcing by 2100. *Climatic Change*, 109(1-2), 77-94. http://doi.org/10.1007/s10584-011-0151-4.

van Giersbergen, N. P. A. (2005). On the effect of deterministic terms on the bias in stable AR models. *Economics Letters*, 89(1), 75-82. http://doi.org/10.1016/j.econlet.2005.05.013.

Vasco, G., Silva, J. S., Canales, F. A., Beluco, A., Souza, J., & Rossini, E. G. (2019). A hydro PV Hybrid system for the Laranjeiras Dam (in Southern Brazil) operating with storage capacity in the water reservoir. *Smart Grid and Renewable Energy*, 10(4), 83-97. http://doi.org/10.4236/sgre.2019.104006.

Wang, F., Shao, W., Yu, H., Kan, G., He, X., Zhang, D., Ren, M., & Wang, G. (2020). Re-evaluation of the power of the Mann-Kendall test for detecting monotonic trends in hydrometeorological time series. *Frontiers in Earth Science*, *8*, 14. http://doi.org/10.3389/feart.2020.00014.

Authors contributions

Gabriel Vasco: Writing - original draft, formal analysis, data curation, conceptualization.

Rodrigo de Queiroga Miranda: Supervision, review & editing, conceptualization, methodology.

Jussara Freire de Souza Viana: Writing - review & editing, conceptualization.

Danielle Bressiani: Review & editing.

Eduardo Mario Mendiondo: Review & editing.

Richarde Marques da Silva: Review & editing.

Josiclêda Domiciano Galvíncio: Review & editing.

Samara Fernanda da Silva: Writing & editing.

Suzana Maria Gico Lima Montenegro: Review & editing, supervision, resources, project administration.

Editor-in-Chief: Adilson Pinheiro

Associated Editor: Carlos Henrique Ribeiro Lima